GeoHealth

RESEARCH ARTICLE

10.1029/2021GH000490

**Key Points:**

- We develop a coupled hydrodynamic, a pathogen, and swimmer illness model to evaluate US/MX border region shoreline wastewater impacts
- Year 2017 model simulations quantitatively assess the benefits of four infrastructure scenarios that reduce regional wastewater inputs
- Tourist season has the most ill swimmers from plumes advecting north from MX, and mitigating this source yields the largest benefit

**Correspondence to:**

F. Feddersen,
ffeddersen@ucsd.edu

**Citation:**

Feddersen, F., Boehm, A. B., Giddings, S. N., Wu, X., & Liden, D. (2021). Modeling untreated wastewater evolution and swimmer illness for four wastewater infrastructure scenarios in the San Diego-Tijuana (US/MX) border region. *GeoHealth*, *5*, e2021GH000490. https://doi.org/10.1029/2021GH000490

Received 27 JUL 2021
Accepted 18 OCT 2021

**Author Contributions:**

**Conceptualization:** Falk Feddersen, Alexandria B. Boehm, Sarah N. Giddings, Doug Liden
**Formal analysis:** Falk Feddersen, Alexandria B. Boehm, Sarah N. Giddings, Doug Liden
**Funding acquisition:** Falk Feddersen
**Methodology:** Falk Feddersen, Alexandria B. Boehm
**Software:** Xiaodong Wu
**Writing – original draft:** Falk Feddersen
**Writing – review & editing:** Falk Feddersen, Alexandria B. Boehm, Sarah N. Giddings, Xiaodong Wu, Doug Liden



# Modeling Untreated Wastewater Evolution and Swimmer Illness for Four Wastewater Infrastructure Scenarios in the San Diego-Tijuana (US/MX) Border Region

**Falk Feddersen[1], Alexandria B. Boehm[2], Sarah N. Giddings[1], Xiaodong Wu[1], and Doug Liden[3]**

[1]Scripps Institution of Oceanography, UCSD, La Jolla, CA, USA, [2]Dept Civil and Environmental Engineering, Stanford University, Stanford, CA, USA, [3]Environmental Protection Agency, San Diego, CA, USA

**Abstract** The popular beaches of the San Diego-Tijuana (US/MX) border region are often impacted by untreated wastewater sourced from Mexico—via the Tijuana River Estuary (TJRE) and San Antonio de los Buenos outfall at the Pt. Bandera (SAB/PTB) shoreline, leading to impacted beaches and human illness. The US-Mexico-Canada trade agreement will fund border infrastructure projects reducing untreated wastewater discharges. However, estimating project benefits such as reduced human illness and beach impacts is challenging. We develop a coupled hydrodynamic, norovirus (NoV) pathogen, and swimmer illness risk model with the wastewater sources for the year 2017. The model is used to evaluate the reduction in human illness and beach impacts under baseline conditions and three infrastructure diversion scenarios which (Scenario A) reduce SAB/PTB discharges and moderately reduce TJRE inflows or (Scenarios B, C) strongly reduce TJRE in inflows only. The model estimates shoreline untreated wastewater and NoV concentrations, and the number of NoV ill swimmers at Imperial Beach CA. In the Baseline, the percentage of swimmers becoming ill is 3.8% over 2017, increasing to 4.5% during the tourist season (Memorial to Labor Day) due to south-swell driven SAB/PTB plumes. Overall, Scenario A provides the largest reduction in ill swimmers and beach impacts for the tourist season and full year. The 2017 tourist season TJRE inflows were not representative of those in 2020, yet, Scenario A likely still provides the greatest benefit in other years. This methodology can be applied to other coastal regions with wastewater inputs.

**Plain Language Summary** The popular beaches of the San Diego-Tijuana border region are often impacted by Mexican-sourced untreated wastewater leading to beach advisories and human health impacts. There are two principal ocean sources: the Tijuana River Estuary (TJRE) and San Antonio de los Buenos outfall at Pt. Bandera (SAB/PTB). The recent US-Mexico-Canada trade agreement will fund infrastructure projects to reduce untreated wastewater flowing into the ocean. Estimating project benefits requires coupling models, which is challenging and has not previously been performed. We develop such a model to estimate shoreline pathogen concentration and swimmer illness risk for the year 2017 for four scenarios of baseline conditions and three infrastructure diversion scenarios which (Scenario A) reduce SAB/PTB discharges and moderately reduce TJRE inflows or (Scenarios B, C) strongly reduce TJRE inflows only. In the Baseline, the percentage of swimmers becoming ill is 3.8% over the year, increasing to 4.5% for the tourist season (Memorial to Labor Day) due to south-swell driven SAB/PTB plumes. Overall, Scenario A provides the largest reduction in ill swimmers both for the tourist season and full year relative to Scenarios B and C that only reduce TJRE inflows. This methodology can be applied to other regions where wastewater enters the ocean.

## 1. Introduction

Recreational bathing in lakes and oceans contaminated with untreated wastewater leads to human illness (e.g., Fleisher et al., 1996; Shuval, 2003). In the United States, an estimated 90 million annual cases of waterborne illness (gastrointestinal [GI], ear, eye, respiratory, or skin) occur from recreational contact with contaminated water, costing over $2 billion dollars per year (DeFlorio-Barker, Wing, et al., 2018). The US Clean Water Act mandates wastewater treatment. Thus, urban runoff and rainfall associated stormwater are the principal sources of pathogen pollution in most of the United States (USEPA, n. d.). In Southern California, recreational contact with ocean water contaminated with urban runoff is associated with elevated

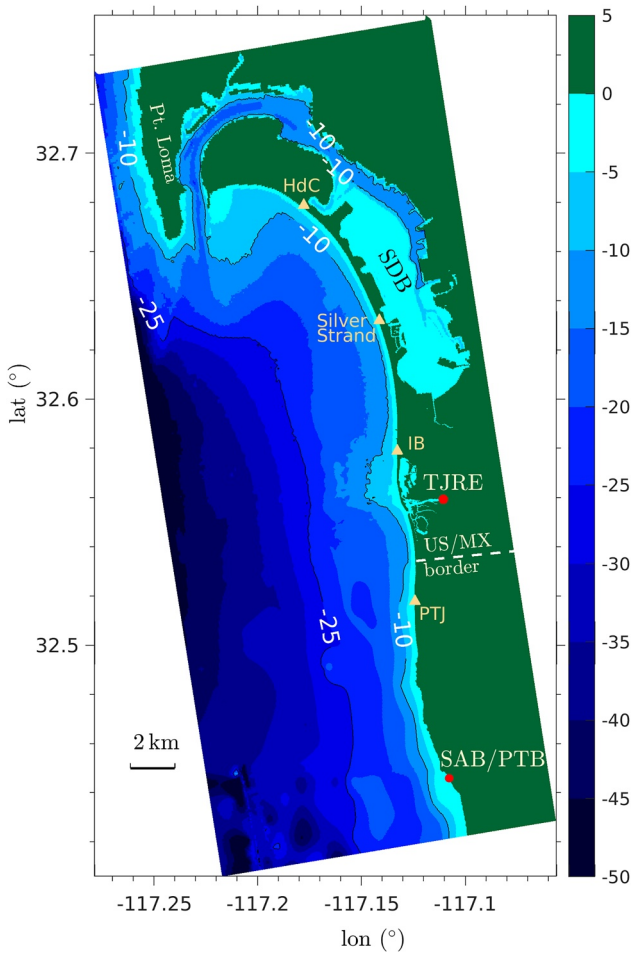


**Figure 1.** San Diego Bight (US/Mexico border region) model domain as a function of latitude and longitude spanning Pt. Loma to south of Punta Bandera (PB) Mexico with bathymetry shown in color. The untreated wastewater sources at the Tijuana River Estuary (TJRE) and the San Antonio de los Buenos outfall located at the shoreline of Punta Bandera (SAB/PTB) are indicated as red dots. Point Loma and the US-Mexico border are labeled. Orange triangles indicate the popular beach locations of Playas Tijuana (PTJ), Imperial Beach (IB), Silver Strand State Beach, and Hotel del Coronado (HdC).

health risk (e.g., Haile et al., 1999). The epidemiological study by Arnold et al. (2017) showed that illness risk associated with coastal seawater contact increases following rainfall events. In countries lacking strict environmental regulations or enforcement, untreated wastewater can be a significant pathogen source to coastal waters. The US/Mexico Pacific Ocean border region, denoted the San Diego Bight (Figure 1) has popular beaches such as the City of Imperial Beach (IB) (US) and Playas Tijuana (MX) which are often under advisories (San Diego County, n. d.) due to poor water quality from principally two untreated wastewater sources to the ocean. With US-Mexico-Canada (USMCA) trade agreement funding, the US EPA Border Water Infrastructure Program is developing infrastructure projects to reduce human illness and beach closure impacts of untreated wastewater sources to the San Diego Bight. The study goal is to develop a coupled hydrodynamic, pathogen, and human illness model to provide scientifically grounded estimates on the reduction of swimmer illness risk and number of beach advisories for four proposed infrastructure scenarios.

The first untreated wastewater source is the binational Tijuana River (ARCADIS, 2019), which flows into the Tijuana River Estuary (TJRE) and subsequently reaches the coastal ocean at the TJRE mouth, ~2 km north of the US/MX border. During dry weather, river flows in Tijuana (MX) consist of a mix of treated and untreated wastewater which is diverted to the International Wastewater Treatment Plant (ARCADIS, 2019). However, with rainfall, diversion is often suspended due to issues with Tijuana infrastructure allowing wastewater to enter the Tijuana River (ARCADIS, 2019). Plumes from the TJRE can hug the shoreline or extend ~20 km offshore (Lahet & Stramski, 2010; Warrick et al., 2007) as a mixture of runoff and untreated wastewater (Ayad et al., 2020). TJRE plumes can impact the entire San Diego Bight particularly during winter when rainfall is more likely to occur (e.g., Kim et al., 2009). A second untreated wastewater source is at the shoreline of Pt. Bandera (PTB—10 km south of the border) serving as the outfall of the San Antonio de los Buenos (SAB) treatment plant. SAB/PTB shoreline discharge is estimated at 40–52 MGD, of which at most 10 MGD are treated due to lack of facility maintenance (ARCADIS, 2019). Informal reports and in person author visits to SAB indicate that SAB treatment capacity was zero and that SAB is completely bypassed. SAB/PTB discharge to the ocean shoreline is associated with elevated fecal indicator bacteria (FIB) levels (Orozco-Borbón et al., 2006), adenoviruses and enteroviruses (Sassoubre et al., 2012). Shoreline sampling from SAB/PTB northward demonstrates that, for multiple digital PCR and DNA-sequenced microbial parameters, wave-driven surfzone currents can transport SAB/PTB water up to 20 km northward (Zimmer-Faust et al., 2021), consistent with surfzone dye studies (Grimes et al., 2020, 2021; Hally-Rosendahl et al., 2015) and models (Wu et al., 2020). The two untreated wastewater sources result in poor shoreline water quality leading to advisories to regional beaches (San Diego County, n. d.). Web based surveys (Brophy, 2016) indicate that regular bathers in IB CA are more likely to have bathing induced-illness than occasional bathers. Although bathing in untreated wastewater contaminated waters is well known to cause illness (e.g., Boehm & Soller, 2020), there are no epidemiological studies of the human health impacts from these untreated wastewater sources.

The oceanic transport and dispersion of untreated wastewater is important for determining shoreline pathogen concentrations. Tracer released from small coastal inlets can be surfzone entrained or jet offshore onto the shelf (Feddersen et al., 2016; Kastner et al., 2019; Olabarrieta et al., 2014; Rodriguez et al., 2018; Wong et al., 2013). Surfzone tracer is often alongshore transported 10 km $d^{-1}$ (Grant et al., 2005; Grimes et al., 2020, 2021), driven by obliquely incident breaking waves. Coupled wave and circulation hydrodynamic

models can concurrently simulate the three-dimensional (3D) flow of estuaries, the breaking-wave driven surfzone, and the shelf (e.g., Kumar et al., 2015, 2012; Olabarrieta et al., 2011; Wu et al., 2020). Hydrodynamic models have previously been coupled to FIB (e.g., *E. coli* [EC] or *Enterococcus* [ENT]) models, particularly in lake systems (e.g., Weiskerger & Phanikumar, 2020). For example, sunlight, temperature, and sedimentation induced FIB loss was coupled to a two-dimensional (2D) hydrodynamic model to simulate EC and ENT in southern Lake Michigan over a month (Liu et al., 2006). Using more complex 3D hydrodynamic models, modeled and observed EC agreed well in Lake St. Clair during Summer 2010 (Madani et al., 2020). In marine environments, 2D and 3D hydrodynamic models coupled to ENT models reproduce diel and tidal ENT fluctuations inside Key Biscane FL (Feng et al., 2013) and effluent plumes near Waikiki HI (Johnson et al., 2013). Beach swimmers become ill by ingesting pathogen-laden seawater. Dose-response quantitative microbial risk assessment (QMRA) models can estimate the probability of swimmer illness due to pathogen exposure for many pathogens including *Salmonella*, *Campylobacter*, *Giardia*, norovirus (NoV), and adenovirus (e.g., Boehm & Soller, 2020; Schoen & Ashbolt, 2010).

Here, we couple hydrodynamic (estuary, surfzone, shelf), pathogen (NoV), and QMRA models (Section 2) to predict pathogen concentration and swimmer illness risk for the year 2017 in the San Diego Bight under four infrastructure scenarios. Although untreated wastewater has a variety of pathogens which lead to human illness (Dorevitch et al., 2012), the model focuses on NoV as it contributes the most to swimmer illness risk based on QMRA simulations (e.g., Boehm & Soller, 2020). The first scenario is a baseline representing no infrastructure change. The other three scenarios reduce either flows into the TJRE or SAB/PTB discharges to the ocean shoreline. For the four scenarios, the shoreline concentration of untreated wastewater is examined over 30 km alongcoast and the number of ill swimmers at IB are simulated (Section 3). In the Discussion (Section 4), we estimate the fraction of time that regional beaches would be under beach water quality advisory for the four scenarios, contextualize the results, discuss the representativeness of year 2017, and model limitations. Section 5 is a summary.

## 2. Methods

### 2.1. Hydrodynamic and Pathogen Model Background

The San Diego Bight model ($15 \times 36$ km$^2$) simulates the estuary, surfzone, and shelf circulation and untreated wastewater transport using the Coupled Ocean-Atmosphere-Wave-Sediment-Transport (COAWST) model system (Kumar et al., 2012; Warner et al., 2010) by coupling the Regional Ocean Modeling System (Shchepetkin & McWilliams, 2005) with the Simulating WAves Nearshore model (Booij et al., 1999). The model spans the San Diego/Tijuana Border region including the San Diego Bay, TJRE, and the SAB outfall at the shoreline of Punta Bandera (SAB/PTB) located at 32.446°N, 10 km south of the US/Mexico border (see Figure 1). We have previously applied the COAWST model in the San Diego Bight, resolving the processes leading to cross-shelf tracer transport that dilutes the shoreline (Wu et al., 2020). Here, only relevant hydrodynamic model background is provided. A full model description is found in Wu et al. (2020) and application is found elsewhere (Wu et al., 2021a, 2021b). The regional shoreline is relatively straight, except for curvature to the north around Coronado near the San Diego Bay entrance and a broad 15 m depth shoal offshore of the TJRE mouth. The horizontal grid resolution transitions from 100 m along the open boundaries to 8 m approaching the TJRE mouth allowing the estuary and surfzone to be resolved. Following seasonal rainfall, the model accounts for realistic freshwater inflows as well as untreated wastewater inflows where the Tijuana River enters the TJRE. The model also accounts for continuous freshwater flows and untreated wastewater flows released at the shoreline of SAB/PTB. These sources are described in Section 2.2. Three one-way nested parent runs spanning from the California Current System to the south Southern California Bight, provide ocean boundary conditions for the San Diego Bight model. The Coastal Data Information Program provides wave boundary conditions. NOAA/NAM surface fluxes (wind stress, heat and precipitation) are applied.

The San Diego Bight model evolves a passive tracer representing untreated wastewater concentration $D$ such that $D = 1$ is pure untreated wastewater. With only one tracer, we are limited to representing only one pathogen. NoV is chosen because, based on QMRA models, it dominates swimmer illness risk from swimming in untreated wastewater contaminated waters (Boehm & Soller, 2020), particularly for aged sewage (Schoen et al., 2020). This is because of its abundance in untreated wastewater (Eftim et al., 2017), being

**Table 1**
*Description of Tijuana River Estuary (TJRE) Freshwater Diversion Limits and San Antonio De Los Buenos Outfall at the Pt. Bandera (SAB/PTB) Wastewater Discharges to the Ocean Shoreline for the Four Modeling Scenarios*

| Scenario | TJRE diversion limit | SAB/PTB wastewater input |
|---|---|---|
| Baseline | 2 MGD (0.09 $m^3 s^{-1}$) | Untreated 35 MGD (1.53 $m^3 s^{-1}$) |
| Scenario A | 35 MGD (1.53 $m^3 s^{-1}$) | Treated 10 MGD (0.44 $m^3 s^{-1}$) |
| Scenario B | 100 MGD (4.38 $m^3 s^{-1}$) | Untreated 35 MGD (1.53 $m^3 s^{-1}$) |
| Scenario C | 163 MGD (7.14 $m^3 s^{-1}$) | Untreated 35 MGD (1.53 $m^3 s^{-1}$) |

*Note*. TJRE inflows beyond these limits are not diverted and enter the TJRE. For SAB/PTB, treated wastewater is assumed to have 5% of the NoV pathogen load of untreated wastewater (e.g., Pouillot et al., 2015; Sano et al., 2016). NoV, norovirus.

long-lived in seawater (unlike EC and ENT) with a median decay constant of $\approx 0.1\ d^{-1}$ (10-day decay time-scale) based on data available to date (e.g., Boehm et al., 2015, 2019), and its low infectious dose. Effects of sunlight, turbidity, and sedimentation, which can be important controls on FIB fate (e.g., Weiskerger & Phanikumar, 2020), are not considered here for NoV. Thus, with specified source NoV concentration $C_{src}$ (copy $L^{-1}$), the shoreline NoV concentration is $C = DC_{src}$. Values of $C_{src}$ are discussed in Section 2.5.

The simulation is conducted from December 12, 2016 12:00 UTC to December 20, 2017 12:00 UTC and solutions are saved at 1-hr intervals. Model output is analyzed from December 15, 2016 12:00 UTC up to December 15, 2017 12:00 UTC (denoted year 2017) allowing for 3 days of model spinup. Analysis is also performed comparing the tourist (dry) season, and wet season. The tourist season is defined as 22 May to 8 September, spanning 109 days from the earliest Memorial Day and latest Labor Day Holidays, consistent with County of San Diego and City of IB CA definitions. The wet season is defined as 1 October to 1 April (spanning 189 days), consistent with State of California definitions.

### 2.2. Scenarios for Freshwater and Untreated Wastewater Input at TJRE and SAB/PTB

Freshwater and untreated wastewater are input into the model domain at the TJRE inflow and SAB/PTB discharge locations (red dots in Figure 1). We have four modeling scenarios that represent a Baseline scenario and three scenarios (A, B, C) where TJRE inflows or SAB/PTB discharges to the ocean shoreline are modified. The three scenarios represent USMCA infrastructure proposals developed by the EPA and reported in various stakeholder meetings to reduce pollution input to the coastal ocean (USEPA, n.d.). These scenarios differ in how much freshwater, including untreated wastewater, flows into the TJRE and how much untreated or treated wastewater is discharged to the ocean shoreline at SAB/PTB as summarized in Table 1.

To represent model TJRE inflows in the Baseline, TJRE freshwater input matches the volume flux $Q_f$ of the International Boundary Water Commission (IBWC) flow gauge located $\approx 4$ km upstream in the Tijuana River. Flows <2 MGD (0.09 $m^3 s^{-1}$) are assumed to infiltrate and not enter the TJRE, thus any $Q_f < 0.09\ m^3 s^{-1}$ are zeroed out. Very high flow rates can lead to model instability. Thus, occasional episodic flows >3000 MGD (132 $m^3 s^{-1}$) are capped and distributed in time to maintain total volume entering the TJRE. Baseline TJRE inflows ≤23 MGD ($Q_f < 1.01\ m^3 s^{-1}$) are assumed to contain 25% untreated wastewater (ARCADIS, 2019), thus untreated wastewater flux is $Q_D = 0.25 Q_f$. Flows greater than 23 MGD are assumed to contain 10 MGD ($Q_D = 0.44\ m^3 s^{-1}$) of untreated wastewater regardless of flow rate. These untreated wastewater assumptions are based on analysis of the Tijuana wastewater infrastructure and how much capacity exists within the system (ARCADIS, 2019). The assumptions are based on "normal" conditions and do not consider catastrophic Tijuana wastewater infrastructure problems leading to untreated wastewater release into the Tijuana River, such as occurred during winter 2017 (IBWC, 2017) and from November 2019 through summer 2020 (IBWC-Data, n.d.). SAB/PTB (Figure 1) discharges between 40 and 52 MGD to the ocean shoreline 10 km south of the border, of which 10 MGD to 0 MGD are treated (e.g., ARCADIS, 2019). Thus, the Baseline model SAB/PTB freshwater discharge is chosen to be constant at 50 MGD ($Q_f = 2.19\ m^3 s^{-1}$) of which 35 MGD (or $Q_D = 1.53\ m^3 s^{-1}$) is untreated wastewater, and the remaining 15 MGD are freshwater (i.e., no pathogens). This spans the potential range of fresh and untreated wastewater discharges.

Three scenarios (A, B, C) modify the TJRE inflows and SAB/PTB discharges to the ocean shoreline as summarized in Table 1 and are representative of potential USMCA-funded infrastructure projects. Scenario A moderately diverts TJRE inflows up to 35 MGD (i.e., only flows > 35 MGD enter the TJRE) and reduces SAB/PTB wastewater discharges to the ocean shoreline to 10 MGD ($Q_D = 0.44\ m^3 s^{-1}$) of treated wastewater. SAB/PTB is designed to use lagoon treatment with partial chlorination. Meta-analysis shows that NoV reduction in lagoon treatment systems without chlorine is −1 log10 (Sano et al., 2016) and with chlorine is −1.5 log10 (Pouillot et al., 2015). Thus, treated wastewater is assumed to have a −1.3 log10 reduction in NoV (i.e., 5%) relative to untreated wastewater. Scenarios B and C only impact freshwater flows into

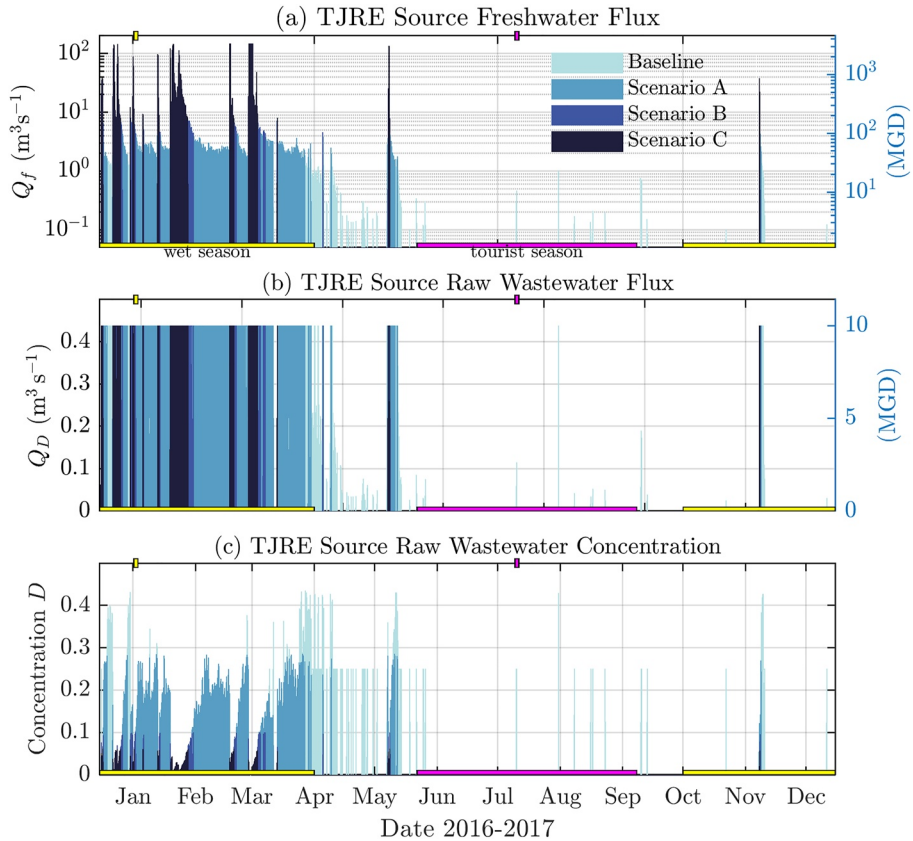


**Figure 2.** Timeseries of Tijuana River Estuary (TJRE) inputs over the year 2017 (December 15, 2016 to December 15, 2017) for the four scenarios: (a) freshwater flux $Q_f$ (m$^3$ s$^{-1}$) and (right) million gallons per day MGD, (b) untreated wastewater flux $Q_D$ (m$^3$ s$^{-1}$), and (c) resulting source untreated wastewater concentration $D$. Colors indicate the Baseline, Scenario A (35 MGD diversion limit), Scenario B (100 MGD diversion limit), and Scenario C (163 MGD diversion limit) as indicated in the legend (see also Table 1). A scenario color is only shown if the diversion limit is exceeded. Thus, a time-period with Scenario C inflows (darkest blue) also have identical inflows for all Scenarios. However, a time period of Scenario A inflows, has identical Baseline inflows, but no Scenario B or C inflows. At the bottom of all panels, magenta and yellow bars indicate the tourist season (22 May to 8 September) and wet season (1 October to 1 April), respectively. Yellow and magenta markers at the top of each panel indicate the time of the wet and tourist season examples (Figure 4).

the TJRE by adjusting the TJRE diversion limits to 100 MGD and 163 MGD, respectively, but leave SAB/PTB discharges identical to the Baseline.

The freshwater flux, the untreated wastewater flux, and untreated wastewater concentration entering the TRJE from the Tijuana River under the four scenarios are shown hourly in Figure 2 and yearly statistics in Table 2. We discuss the Baseline first. During the early wet season (December 2016–March 2017), the Baseline TJRE freshwater flux is nearly always above $Q_f > 1$ m$^3$ s$^{-1}$ and can be large, up to 100 m$^3$ s$^{-1}$ (Figure 2a). During the early wet season with consistently elevated $Q_f > 1$ m$^3$ s$^{-1}$, Baseline untreated wastewater flux is capped at 10 MGD ($Q_D = 0.44$ m$^3$ s$^{-1}$, Figure 2b), resulting in source untreated wastewater concentrations that vary from $D = 0.44$ for weak $Q_f$ to $D = 0.02$ for the strongest $Q_f$ (Figure 2c). During the tourist (dry) season, $Q_f$ is minimal with episodic short-duration events on average $Q_f = 0.2$ m$^3$ s$^{-1}$ but up to 1 m$^3$ s$^{-1}$ (Figure 2a) and associated untreated wastewater flux from $Q_D = 0.05$ m$^3$ s$^{-1}$ to 0.4 m$^3$ s$^{-1}$ (Figure 2b). In the later 2017 wet season (October–December 2017), $Q_f$ and $Q_D$ are similar to the tourist season except for a large early November event (Figure 2). Over the year, the Baseline has nonzero hourly TJRE input 48% of the time with net freshwater and untreated wastewater inputs totaling $94.6 \times 10^6$ m$^3$ and $3.9 \times 10^6$ m$^3$, respectively (Table 2).

**Table 2**
*For the Four Scenarios, Tijuana River Estuary (TJRE) Freshwater and Untreated Wastewater Input Volume ($m^3$), the Percentage of Time TJRE $Q_f$ Is Nonzero, and the San Antonio De Los Buenos Outfall at the Pt. Bandera (SAB/PTB) Untreated Wastewater Discharge Volume (Input) Over the Full Year December 15, 2016 12:00 UTC to December 12, 2017 12:00 UTC*

| Year TJRE input | Baseline | Scenario A | Scenario B | Scenario C |
|---|---|---|---|---|
| Freshwater ($\times 10^6$ $m^3$) | 94.6 | 93.5 | 79.8 | 76.0 |
| Untreated wastewater ($\times 10^6$ $m^3$) | 3.9 | 3.6 | 1.2 | 0.9 |
| Percentage time $Q_f > 0$ | 49% | 39% | 12% | 9% |
| SAB/PTB untreated wastewater input ($\times 10^6$ $m^3$) | 48.3 | 0.7 | 48.3 | 48.3 |

*Note*. The wet season provides >99.7% and ≥99.1% of the yearly total baseline TJRE freshwater and untreated wastewater input, respectively. Scenarios A–C have zero TJRE input during tourist season.

We next examine the associated TJRE $Q_f$ and $Q_D$ for Scenarios A, B, and C (Table 1). Scenario A (diverting inflows <35 MGD) eliminates all TJRE inflows during tourist season and some of the weaker $Q_f$ flows during late March through May (Figures 2a and 2b). The yearly percentage of time that Scenario A $Q_f > 0$ is 39% reduced from Baseline 49% (Table 2). However, because the early wet season $Q_f$ (and $Q_D$) are typically strong, Scenario A reduces the net yearly TJRE freshwater and untreated wastewater input only 2% and 8%, respectively, from the Baseline (Table 2). Scenarios B and C eliminate many times of nonzero $Q_f$, particularly in the early wet season, such that nonzero TJRE $Q_f$ only occurs 12% and 9% of the time, respectively. However, Scenarios B and C still have a number of episodic strong (>163 MGD) flow events associated with strong precipitation that typically lead to low input $D$ (Figure 2). Because TJRE $Q_f$ is typically episodic, mostly <100 MGD with occasional events well over 163 MGD, the yearly freshwater input for both Scenarios B and C are similar and reduced ≈18% from the baseline (Table 2) as most of the yearly $Q_f$ is from a few very large events. Because with our input assumptions $Q_D$ is capped at 0.44 $m^3$ $s^{-1}$ (10 MGD), regardless of $Q_f$ magnitude, Scenarios B and C yearly untreated wastewater inflows to the TJRE are similar and are reduced 69% and 77% from the Baseline, respectively. Note, overall SAB/PTB untreated wastewater discharges are much larger than for those of the TJRE, and the Scenario A SAB/PTB input is less than the Scenario C TJRE input (Table 2).

### 2.3. Shoreline Untreated Wastewater Concentration and Locations of Interest

Simulated shoreline untreated wastewater concentrations $D$ are extracted over a 31 km alongcoast distance from the southern model boundary northward, accounting for coastline curvature. With ±1 m tidal variation, at each alongcoast grid point every 10–60 m, the most onshore location where the tidal water depth was at least 1 m is used to represent the shoreline $D$. At the TJRE mouth, the shoreline is virtually extended so as to not select locations within the estuary. Distance alongcoast is represented by $y$ and is given relative to the City of IB Pier (located at 32.579°N). Specific locations of interest are are shown in Figures 1, 4 and 5, including SAB/PTB ($y = -15.3$ km), the TJRE mouth ($y = -2.9$ km), the US/Mexico Border, and four popular regional beaches: (from south to north) Playas Tijuana Mexico (PTJ, $y = -6.9$ km), IB Pier, Silver Strand State Beach (SS, $y = 6$ km), and the Hotel del Coronado (HdC, $y = 12.1$ km), located within the City of Coronado.

### 2.4. City of IB CA Beach Attendance

City of IB monthly beach attendance records, compiled by lifeguards, were obtained for the years 2014–2019 (City of IB, pers communication). The monthly data were averaged over the six years and interpolated to obtain hourly beach visitors such that the sum of hourly beach visitors equaled the yearly total beach visitors of 2.4 million. Beach visitor variation within a week (intra-week) or within a day (intra-day) are not included. Thus, beach visits are evenly distributed between day and night and throughout the week. For other Southern California (Los Angeles County and Orange County) beaches that experience similar weather and wave conditions as IB CA. Given et al. (2006) provide the monthly percentage of beach visitors who swim which varies from 10% in February to 43% in August. This monthly fraction is also interpolated

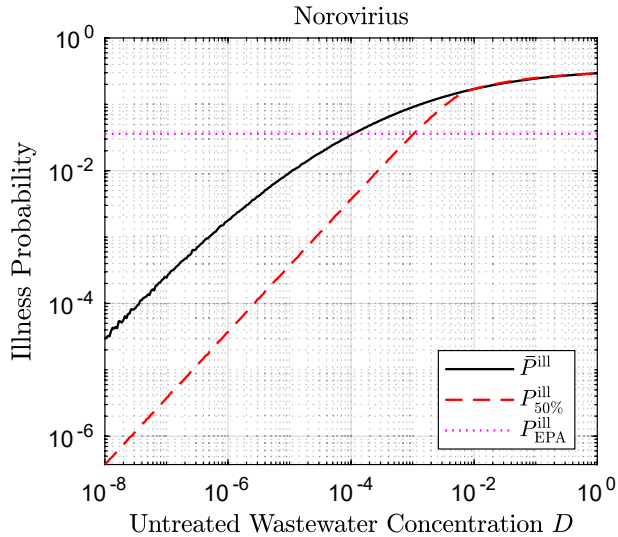


**Figure 3.** $P^{ill}$ versus untreated wastewater concentration $D$ showing expected (mean) probability $\bar{P}^{ill}$, median probability $P^{ill}_{50\%}$, and the EPA threshold $P^{ill}_{EPA} = 0.036$ (USEPA, 2012) as indicated in the legend.

to hourly and used to derive hourly IB swimmers $N_{swim}$. Intra-day or intra-week $N_{swim}$ variations are not included, as the scientific literature does not provide information on how to distribute $N_{swim}$ throughout the day or week. However, $N_{swim}$ clearly varies with time of day, being elevated midday, significantly reduced early morning and late afternoon, and largely zero at night, and likely varies by day of week. The effect of intra-day variations in $N_{swim}$ are explored in Appendix A and do not affect the results.

### 2.5. Estimation of NoV Illness Probability

We estimated the illness risk from NoV exposure with the methods in Boehm and Soller (2020). The modeled untreated wastewater concentration $D$ has a 10 days e-folding decay time-scale (Section 2.1), consistent with the median decay time scale for NoV (Boehm et al., 2019). NoV concentration in source untreated wastewater $C_{src}$ is represented by a random variable with a log10-normal distribution with a log10 mean of 4 and standard deviation of 1.4 such that the mode is $10^4$ copy $L^{-1}$ (Eftim et al., 2017). Swimmers are assumed to ingest a volume of water $V$ (mL) drawn from a log10-normal distribution with a log10 mean of 1.2 and standard deviation of 0.68 (DeFlorio-Barker, Arnold, et al., 2018). For an individual swimmer, the NoV dose $\mu$ is given as

$$\mu = C_{src} DV \tag{1}$$

where $V$ is the volume of water ingested. From Teunis et al. (2008), the NoV probability of infection $P^{inf}$ is a function of the dose $\mu$,

$$P^{inf} = 1 -_1 F_1(0.04, 0.09, -\mu), \tag{2}$$

where $_1F_1$ is the hypergeometric function. The conditional probability of illness given infection $P^{ill|inf}$ is a uniform random variable over [0.3, 0.8] independent of $P^{inf}$ (Teunis et al., 2008) such that the probability of illness

$$P^{ill} = P^{ill|inf} P^{inf}. \tag{3}$$

At the City of IB, the number of hourly ill swimmers $N_{ill}$ is calculated using estimates of the number of hourly swimmers $N_{swim}$ and the shoreline $D$ from December 15, 2016 12:00 UTC to December 15, 2017 12:00 UTC. For a particular hour, each individual swimmer ingests a volume $V$ of water randomly drawn from the distribution described above. Conceptually, we expect that all swimmers at a particular location and hour experience the same NoV concentration $DC_{src}$. Therefore, for a single swimmer we draw $N_c = 250$ random samples of $C_{src}$ to obtain $N_c$ estimates of $\mu_i$ (a) and $N_c$ estimates of $P^{inf}_i$ (b), and $P^{ill}_i$ (c), where $i \in [1, ..., N_c]$. We then draw $N_c$ samples from a uniformly distributed random variable on [0, 1], denoted $R_i$. For each $i$, if $R_i < P^{ill}_i$, then $1/N_c$ of a swimmer is considered ill, and we sum over all $i$. This acts as an ensemble average over possible source NoV concentrations $C_{src}$. Results were not sensitive to increasing $N_c$. This process is repeated for each swimmer within each hour to calculate hourly $N_{ill}$. Note, fractional hourly $N_{ill}$ are possible.

As $C_{src}$ and $V$ are independent random variables, the NoV swimmer illness probability $P^{ill}$ for a value of $D$ has a probability density function with a mean and median. The probability density function of $P^{ill}$ and its dependence on $D$ is estimated by drawing $N_{tot} = 10^5$ independent random values of $C_{src}$, $V$, and $P^{ill|inf}$, resulting in $N_{tot}$ values of $P^{ill}$ for each $D$. From this, we estimate the mean (expected) $\bar{P}^{ill}$ and median $P^{ill}_{50\%}$ illness probability for each possible value of $D$ (Figure 3), representing an ensemble over $C_{src}$ and $V$. From $D = 10^{-2}$ to $D = 1$, $\bar{P}^{ill}$ varies from 0.2 to 0.3. At smaller values of $D < 10^{-2}$, $\bar{P}^{ill}$ decreases in a power-law relationship of $\bar{P}^{ill} \sim D^{0.8}$ such that at $D = 10^{-8}$, $\bar{P}^{ill} = 2 \times 10^{-5}$. At $D > 10^{-2}$, the mean $\bar{P}^{ill}$ and median $P^{ill}_{50\%}$ are the same, indicating that the probability density function is effectively symmetric. However for $D < 10^{-2}$, $P^{ill}_{50\%}$ is smaller than $\bar{P}^{ill}$ such that $\bar{P}^{ill}/P^{ill}_{50\%} \approx 10$ at $D = 10^{-4}$ and $\bar{P}^{ill}/P^{ill}_{50\%} \approx 100$ at $D = 10^{-8}$. This suggests that at very low values of $D$, ill swimmer $N_{ill}$ estimated from $\bar{P}^{ill}$ will be biased high. This will be explored in Section 3.4.

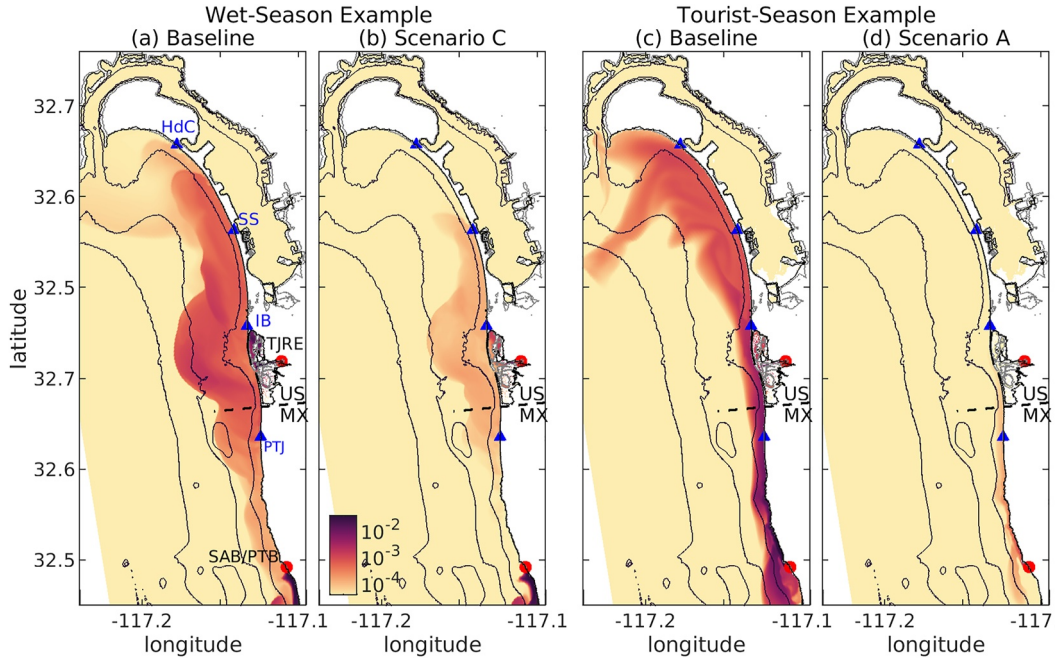


**Figure 4.** (a and b) Wet-season case example from January 3, 2017 10:00 UTC of modeled surface (a) Baseline and (b) Scenario C untreated wastewater concentration $D$. (c and d) Tourist season case example from July 11, 2017 14:00 UTC of modeled surface (c) Baseline and (d) Scenario A untreated wastewater concentration $D$. Red dots indicate locations of Tijuana River Estuary (TJRE) and San Antonio de los Buenos outfall at the Pt. Bandera (SAB/PTB) sources. Blue triangles mark specific beaches: Playas Tijuana (PTJ), Imperial Beach Pier (IB), Silver Strand State Beach (SS), and the Hotel del Coronado (HdC). The dashed line marks the US-Mexico border. These example times are indicated in Figure 2. For the wet season examples (a and b), the TJRE freshwater and untreated wastewater flux (averaged over the preceding 48 hr) are $Q_f = \{4.04, 0.32\}$ m$^3$ s$^{-1}$ and $Q_D = \{0.44, 0.018\}$ m$^3$ s$^{-1}$, respectively for the Baseline and Scenario C. For the tourist season examples (c and d), the TJRE freshwater and untreated wastewater flux (averaged over the preceding 48 hr) are $Q_f = \{0.04, 0\}$ m$^3$ s$^{-1}$ and $Q_D = \{0.01, 0\}$ m$^3$ s$^{-1}$, respectively for the Baseline and Scenario A. Note, in wet season (a and b), Scenario A is very similar to the Baseline and Scenario B is similar with slightly elevated $D$ to Scenario C. In tourist season (c and d), Scenarios B and C are nearly identical to the Baseline.

Here, pathogen concentration limits for determining beach advisories are based on the concentration that results in mean probability of GI illness $P^{\text{ill}}_{\text{EPA}} = 0.0036$ (i.e., 3.6/100) (USEPA, 2012). At $D = 1.06 \times 10^{-6}$, the EPA recreational water quality illness probability threshold $\bar{P}^{\text{ill}} = P^{\text{ill}}_{\text{EPA}} = 0.036$ is crossed (dotted line in Figure 3).

## 3. Results

### 3.1. Example Wet and Tourist Season Untreated Wastewater Plume Events

Here, we show a wet season (winter) and tourist season (dry) San Diego Bight model examples to highlight the untreated wastewater impacts from both TJRE and SAB/PTB sources and the effect of the source reductions from the different scenarios (Figure 4). The wet season example (January 3, 2017 10:00 UTC) has elevated untreated wastewater concentrations ($D > 10^{-3}$) within 2–3 km of shore from south of PTJ northward nearly to HdC (Figure 4a), sourced from the TJRE. The shoreline $D$ varies from $10^{-3}$ at PTJ to around $3 \times 10^{-4}$ from IB to north of SS, and $3 \times 10^{-5}$ at HdC. At these $D$ levels, $\bar{P}^{\text{ill}}$ exceeds the EPA threshold everywhere but HdC. South of SAB/PTB, $D$ is very high ($> 10^{-2}$) from the SAB/PTB source which is advected south. In this wet-season example, Scenario C results in reduced $D$ (Figure 4b) due to the reduced TJRE inflow. Relative to the baseline, the shoreline $D$ is reduced by factor 3–10 from PTJ to SS, corresponding to $\bar{P}^{\text{ill}}$ that just exceeds the EPA threshold, and a factor of 1.5 at HdC. During the wet-season example, Scenario A has no effect on reducing shoreline $D$ and Scenario B results in a factor 2–3 reduction in shoreline $D$ (not shown).

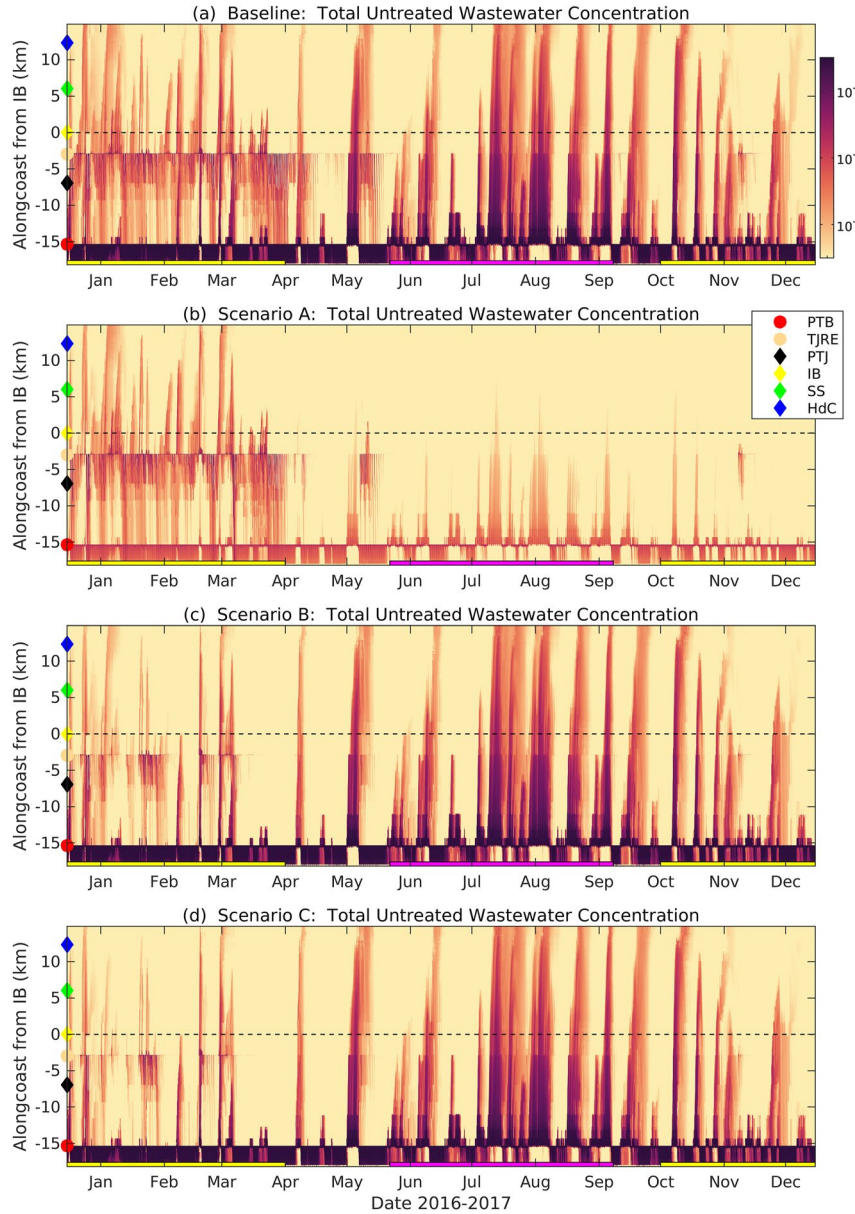


**Figure 5.** Shoreline untreated wastewater concentration $D$ versus time and alongcoast distance from Imperial Beach CA for the (a) Baseline, (b) Scenario A, (c) Scenario B, and (d) Scenario C. The San Antonio de los Buenos outfall at the Pt. Bandera (SAB/PTB) and Tijuana River Estuary (TJRE) sources are indicated on the ordinate as circles. Other alongcoast locations are indicated on the ordinate including Punta Bandera (PTB red), Playas Tijuana (PTJ, black), the mouth of TJRE (magenta), Imperial Beach (IB) pier (yellow, dashed line), Silver Strand State Beach (SS, green), and Hotel del Coronado (HdC, blue). The tourist (22 May to 8 September) and wet (1 October to 1 April) seasons are indicated with magenta and yellow bars, respectively, at the bottom of each panel.

The tourist-season (dry) San Diego Bight model Baseline example (July 11, 2020 14:00 UTC) highlights the impacts of the SAB/PTB source (Figure 4c). Untreated wastewater concentration $D$ is elevated within 1 km of shore along the entire shoreline from SAB/PTB to north of HdC. A strong and long-lived *south swell* (waves incident from the south-southwest) led to strong northward surfzone currents advecting SAB/PTB sourced $D$ northward. The alongshore advection of nearshore SAB/PTB plumes is directly linked to the angle and height of the incident surface gravity waves (Wu et al., 2020). During this dry-weather time, the TJRE input is negligible. The shoreline $D$ varies south to north from $D = 7 \times 10^{-3}$ at PTJ, to $D = 2 \times 10^{-3}$ at IB, $D = 7 \times 10^{-4}$ at SS, and $D = 3 \times 10^{-4}$ and HdC. This corresponds to $\bar{P}^{\text{ill}} = 0.1$ at PTJ to $\bar{P}^{\text{ill}} = 0.05$ at

HdC—all well above the EPA threshold—suggesting negative impacts to regional beaches. For this example, Scenario A dramatically reduces (30–90× relative to the Baseline) $D$ (Figure 4d) due to the significant SAB/PTB source reduction. For example, Scenario A $D = 10^{-4}$ at PTJ, $D = 2.2 \times 10^{-5}$ at IB, and $D \leq 10^{-5}$ at SS and HdC. At these $D$ levels, PTJ $\bar{P}^{ill}$ is right at the EPA threshold and all other locations are below (Figure 3). In contrast, tourist season Scenarios B and C have shoreline $D$ nearly identical to the Baseline (not shown) as they do not alter SAB/PTB discharge.

### 3.2. Shoreline Total Untreated Wastewater Concentration for All Four Scenarios

The wet and tourist season examples highlight the typical transport pathways of the TJRE and SAB/PTB sources, and the effects of TJRE or SAB/PTB source reductions through Scenarios A–C (Figure 4). We examine next shoreline $D$ from SAB/PTB to HdC over the full year (Figure 5) for the Baseline and Scenarios A, B, and C (Table 1 and Figure 2). The Baseline (Figure 5a) highlights the seasonal difference in shoreline $D$ impacts from the TJRE and SAB/PTB sources. During the wet season, the region near the TJRE mouth has consistently elevated $D$ indicating it is the principal regional source from PTJ to HdC. The wet season TJRE outflow is somewhat more likely to go south (due to more prevalent waves from the northwest) impacting PTJ more strongly. Occasionally, weak TJRE-sourced plumes reach HdC at $D \sim 10^{-4}$ with a very short lived maximum of $10^{-3}$. During the wet season, SAB/PTB shoreline $D$ is elevated but mostly flows southward. During occasional south swell events, SAB/PTB sourced $D$ flows northward, impacting PTJ to SS. Overall, the dominant pattern changes in the tourist season (22 May to 8 September) when the SAB/PTB source (Figure 5a) drives many ($\approx$10) tourist-season events with elevated $D$ flowing northward alongcoast from SAB/PTB that last for days. These events propagate generally 8–14 km $d^{-1}$ (see sloping contours in Figure 5a), are associated with south swell events, and dilute relatively slowly alongcoast, leading to significant elevated $D$ from PTJ to the HdC with shoreline $D > 5 \times 10^{-4}$ and nearly always $> 10^{-4}$ . During the tourist season, TJRE $Q_f$ and $Q_D$ are minimal (Figure 2b), indicating that TJRE-inflow impacts are weak.

We next examine the shoreline concentrations for Scenario A (Figure 5b), which eliminates TJRE inflow below 35 MGD and reduces SAB/PTB discharges to 10 MGD of treated wastewater (Table 1). During wet season, the Scenario A shoreline $D$ (Figure 5b) is similar to but somewhat reduced relative to the Baseline (Figure 5a), due to the 20% reduction in TJRE sourced untreated wastewater. However, during the tourist season, Scenario A (Figure 5b) is dramatically different from the Baseline (Figure 5a), with significantly reduced shoreline $D$ from PTJ to HdC due to the strong reduction in the SAB/PTB source. For example, in Scenario A, the tourist season IB maximum shoreline $D = 7 \times 10^{-5}$ almost 100× smaller than the Baseline. Thus, Scenario A reduces tourist season $D$ strongly, but has small impact during the wet season. Scenarios B and C (which only reduce TJRE inflows Table 1 and Figure 2) have similar patterns (Figures 5c and 5d). During the wet season, both scenarios clearly reduce shoreline $D$ substantially relative to the Baseline (Figures 5c and 5d) as the average TJRE inflow $Q_D$ is reduced 71% and 78%, respectively from the Baseline. Three late (February and March) wet-season events have northward flowing SAB/PTB $D$ that impact IB and farther northward (Figures 5c and 5d). In contrast, the tourist season shoreline $D$ for Scenarios B and C are nearly identical to the Baseline (compare Figures 5c and 5d with Figure 5a), as TJRE inflow is negligible and SAB/PTB discharge to the ocean shoreline is unchanged. Thus, Scenarios B and C do not reduce tourist season shoreline $D$ from PTJ to HdC.

### 3.3. IB CA Swimmer Illness Under the Four Scenarios

Throughout the San Diego Bight, shoreline $D$ can be elevated anytime of year (Figure 5), suggesting swimmer illness risk at regional beaches. We now estimate the number of hourly ill swimmers $N_{ill}$ at the City of IB for the four scenarios from the hourly shoreline $D$ and $N_{swim}$ (Section 2.4) using the Boehm and Soller (2020) methods (Section 2.5). During the wet season in the Baseline and Scenario A, IB $D$ is always $> 10^{-5}$ and often $> 10^{-4}$ in 1–3 days duration events (Figure 6a). During the wet season, Scenarios B and C have $D$ reduced by a factor of $\sim$5 and $\sim$10, respectively. During tourist season, the Baseline and Scenarios B and C are essentially identical with $D > 10^{-4}$ regularly in $\approx$7 events of 3–10 days duration (Figure 6a). Scenario A tourist season $D$ is substantially reduced and only 1.5% of the Baseline, consistent with the SAB/PTB discharge reductions. The hourly beach visitors (Section 2.4) varies from $\approx$140 in January to $\approx$700 in July (Figure 6b). The $N_{swim}$ varies from $\approx$14 in January to $\approx$300 in July (dashed in Figure 6b). The annual

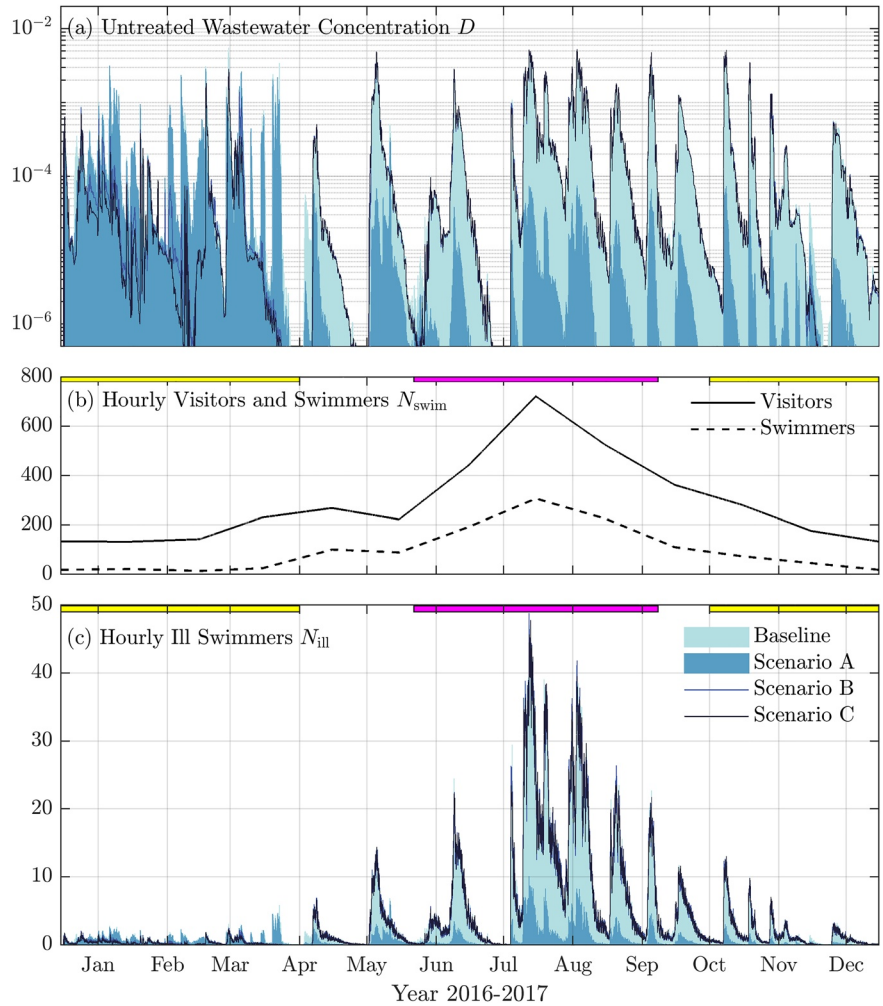


**Figure 6.** Timeseries at Imperial Beach CA of shoreline (a) untreated wastewater concentration $D$, (b) hourly beach visitors and swimmers $N_{swim}$ and (c) hourly ill swimmers $N_{ill}$ for the four scenarios. Panels (a and c) colors correspond to the four scenarios (see legend). The wet and tourist seasons are indicated with yellow and magenta bars at top of panels (b and c). In panel (a), $D$ is extracted along the dashed line in Figure 5. Note, during most of the tourist season, Scenario B and C are nearly identical to each other (and to the Baseline) leading to indistinguishable lines. Similarly during the wet season, Scenario A results in only slightly lower $D$ and $N_{ill}$ relative to the Baseline which is nearly indistinguishable.

swimmer total is 839,784 with 64% during tourist season, 17% during wet season, and the remaining 19% between (Table 3). During the tourist season when $N_{swim}$ is large, elevated $D$ events (Figure 6a) result in large Baseline $N_{ill}$ (Figure 6c), often exceeding 20 and as large as 50, with variability linked to both $D$ and $N_{swim}$. For example, when $D > 10^{-4}$ and $N_{swim} > 100$, then $N_{ill} \geq 10$. During tourist season, Scenario A has substantially reduced $N_{ill}$ relative to the Baseline and Scenarios B and C (Figure 6c). During early wet-season, $N_{ill}$ is generally small due to the reduced $N_{swim}$ with Scenario C having the smallest $N_{ill}$ (Figure 6c). During the late wet-season, a few northward flowing SAB/PTB plumes result in three October $N_{ill}$ events (i.e., $N_{ill} > 5$ that lasts 2–5 days) which are only reduced in Scenario A.

The estimated impact of untreated wastewater on human illness under the four scenarios is quantified for the full year, wet season, and tourist season (Table 3). For the full year, the Baseline $N_{ill} \approx 34,000$ representing 3.8% of $N_{swim}$. Scenario A reduces $N_{ill}$ substantially over the full year so $N_{ill}$ is only 0.6% of $N_{swim}$. Scenarios B and C result in only small (≈1000 or 0.1%) yearly reductions in $N_{ill}$ relative to the Baseline. The wet season has 17% of the yearly $N_{swim}$, and $N_{ill}$ is 2.8% of $N_{swim}$ in the Baseline, which is reduced to 2.2% and 2.1% in Scenarios B and C, respectively (Table 3). However, Scenario A results in the largest wet-season

**Table 3**
*Imperial Beach CA Hourly Swimmers $N_{swim}$ and Ill Swimmers $N_{ill}$, With Ill Swimmer Percentage in Parentheses Under the Four Scenarios for the (Rows) Full Year, Wet Season, and Tourist Season*

| | | Full year | Wet season | Tourist season |
|---|---|---|---|---|
| | Swimmers $N_{swim}$ | 893,784 | 153,747 | 568,152 |
| $N_{ill}$ (percentage) | Baseline | 34,271 (3.8%) | 4,368 (2.8%) | 25,750 (4.5%) |
| | Scenario A | 5,674 (0.6%) | 1,882 (1.2%) | 3,111 (0.5%) |
| | Scenario B | 33,172 (3.7%) | 3,418 (2.2%) | 25,706 (4.5%) |
| | Scenario C | 33,013 (3.7%) | 3,241 (2.1%) | 25,694 (4.5%) |
| $\bar{P}^{ill} N_{swim}$ (percentage) | Baseline | 34,413 (3.9%) | 4,418 (2.9%) | 25,794 (4.5%) |
| | Scenario A | 5,763 (0.6%) | 1,939 (1.3%) | 3,131 (0.6%) |
| | Scenario B | 33,182 (3.7%) | 3,454 (2.2%) | 25,686 (4.5%) |
| | Scenario C | 33,055 (3.7%) | 3,288 (2.1%) | 25,685 (4.5%) |
| $P^{ill}_{50\%} N_{swim}$ (percentage) | Baseline | 11,829 (1.3%) | 1,127 (0.7%) | 9,687 (1.7%) |
| | Scenario A | 555 (0.1%) | 355 (0.2%) | 162 (0.0%) |
| | Scenario B | 11,526 (1.3%) | 859 (0.6%) | 9,668 (1.7%) |
| | Scenario C | 11,485 (1.3%) | 822 (0.5%) | 9,651 (1.7%) |

*Note*. The middle rows have ill swimmers calculated from $N_{swim}\bar{P}^{ill}$ (see Figure 6) and the percentage in parentheses. The bottom rows have ill swimmers calculated from the median probability $N_{swim}P^{ill}_{50\%}$ (with percentage). Note that ill swimmers are rounded to the nearest integer.

$N_{ill}$ reduction with $N_{ill}$ only 1.2% of $N_{swim}$, due to the three October $N_{ill}$ events (Figure 6c). Although October is within the wet season, it is often dry with negligible TJRE inflow (Figure 2a) and can have south swell events driving SAB/PTB plumes northward alongcoast (e.g., Figure 4c). Tourist season has the majority of $N_{swim}$, and $N_{ill}$ is 4.5% of $N_{swim}$ in the Baseline, which is essentially unchanged in Scenarios B and C. Scenario A dramatically reduces $N_{ill}$ during the Tourist season with $N_{ill}$ 0.5% of $N_{swim}$ (Table 3). Overall, Scenario A results in the smallest number of ill swimmers over the full year, tourist season, and wet season.

### 3.4. Representing Number of Ill Swimmers Using Mean and Median Illness Probability: Sensitivity Analysis

The results of Section 3.3 allows for the calculation of hourly or daily $N_{ill}/N_{swim}$, and if this exceeds $P^{ill}_{EPA} = 0.036$ (i.e., 3.6/100), EPA guidelines dictate posting a beach advisory (USEPA, 2012). In many cases, $N_{swim}$ data are unavailable precluding such a calculation. However, if $N_{swim}$ is large enough such that the full $P^{ill}$ distribution is sampled, then $N_{ill}$ will be well approximated by $\bar{P}^{ill}N_{swim}$, where $\bar{P}^{ill}$ is the mean $P^{ill}$ (Figure 3). However, as the $P^{ill}$ distributions are skewed (Figure 3), $N_{swim}$ may not be large enough, such that using $\bar{P}^{ill}$ may create a bias. Here, we explore how well $N_{ill}$ can be estimated using $\bar{P}^{ill}N_{swim}$ for the Baseline (largest $N_{ill}$) and Scenario A (smallest $N_{ill}$).

Using the $D$–$\bar{P}^{ill}$ relationship (Figure 3), $\bar{P}^{ill}$ is estimated at IB from shoreline $D$ for all four scenarios (Figure 7a). The Baseline mean illness probability $\bar{P}^{ill}$ varies from $5.8 \times 10^{-5}$ to 0.15, qualitatively similar to the Baseline $D$. For the other scenarios, $\bar{P}^{ill}$ varies qualitatively similar to their respective $D$. During the wet season, Scenario A $\bar{P}^{ill}$ is similar to the Baseline, but during the tourist season, Scenario A $\bar{P}^{ill}$ is reduced by a factor ≈10 relative to the Baseline. During the wet season, Scenarios B and C have reduced $\bar{P}^{ill}$ except during intermittent flows too strong to be diverted. During the tourist season, Baseline and Scenarios B and C $\bar{P}^{ill}$ are largely identical.

We next compare the $N_{ill}$ against $\bar{P}^{ill}N_{swim}$. The hourly $N_{ill}$ is well represented by $\bar{P}^{ill}N_{swim}$ in both the Baseline and Scenario A during both wet and tourist seasons (Figures 7b and 7c). Over the full year, the $N_{ill}$ and $\bar{P}^{ill}N_{swim}$ have squared correlation > 0.97 and root-mean-square error ≈ 0.6 ill swimmer in both the Baseline and Scenario A (Figure 7). When summed over the wet season, tourist season, or full year, the $N_{ill}$ and $\bar{P}^{ill}N_{swim}$ are very similar in all four scenarios over wet season, tourist season, or the full year, deviating

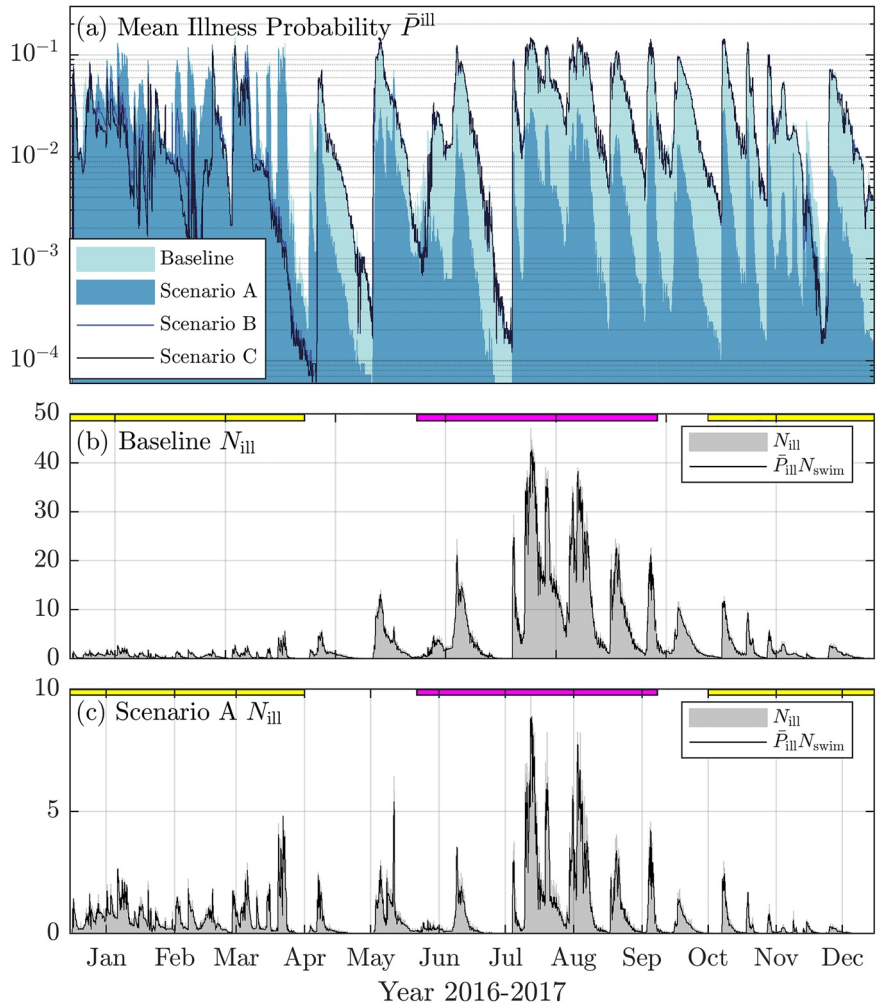


**Figure 7.** Timeseries at Imperial Beach CA of (a) mean norovirus illness probability $\bar{P}^{ill}$ for the four scenarios (legend) and (b and c) number of hourly ill swimmers $N_{ill}$ and $\bar{P}^{ill} N_{swim}$ (see legend) for (b) the Baseline and (c) Scenario A. Yellow and magenta bars at the top of panels (b and c) indicate the wet and tourist seasons. In (a) during most of tourist season, Scenarios B, C, and Baseline $\bar{P}^{ill}$ are nearly identical. Similarly, during the wet season, Scenario A and Baseline $\bar{P}^{ill}$ are very similar and thus nearly indistinguishable. In the Baseline (b), the squared correlation $r^2 = 0.99$ and the root-mean-square error (rmse) is 0.61 hourly swimmers over the full year between $N_{ill}$ and $\bar{P}^{ill} N_{swim}$. Similarly, for Scenario A (c), the squared correlation $r^2 = 0.97$ and the rmse is 0.57 over the full year. For reference, using $P^{ill}_{50\%} N_{swim}$ in (b and c) yields $r^2$ of 0.62 and 0.39 and rmse of 4.6 and 4.6, respectively.

by no more that 0.1% of the total $N_{swim}$ (Table 3). Thus, $\bar{P}^{ill} N_{swim}$ well represents $N_{ill}$ across all scenarios and seasons.

Median illness probability $P^{ill}_{50\%}$ also often is used in illness-risk studies (e.g., Boehm & Soller, 2020), and we explore how well $N_{ill}$ is estimated using $P^{ill}_{50\%} N_{swim}$. As before, $P^{ill}_{50\%}$ is estimated at IB for all four scenarios using the $D$-$P^{ill}_{50\%}$ relationship (Figure 3). For both Baseline and Scenario A, the $N_{ill}$ and $P^{ill}_{50\%} N_{swim}$ squared correlation (0.62 and 0.39) and rmse (≈ 4.6 ill swimmers) indicate $\bar{P}^{ill}$ is better than $P^{ill}_{50\%}$ for estimating $N_{ill}$. In addition, $P^{ill}_{50\%} N_{swim}$ is biased low relative to $N_{ill}$. Over the wet season, tourist season, or full year (Table 3), the Baseline full year $P^{ill}_{50\%} N_{swim}$ only 1/3 of $N_{ill}$ with analogous bias in other scenarios. The low bias in $P^{ill}_{50\%} N_{swim}$ is smallest during tourist season when $N_{swim}$ is largest. These results indicate that $P^{ill}$ distribution is well sampled even for $N_{swim} \approx 20$ and that $\bar{P}^{ill}$ can be used to estimate the hourly $N_{ill}/N_{swim}$. In contrast, using $P^{ill}_{50\%}$ leads to biased low results.

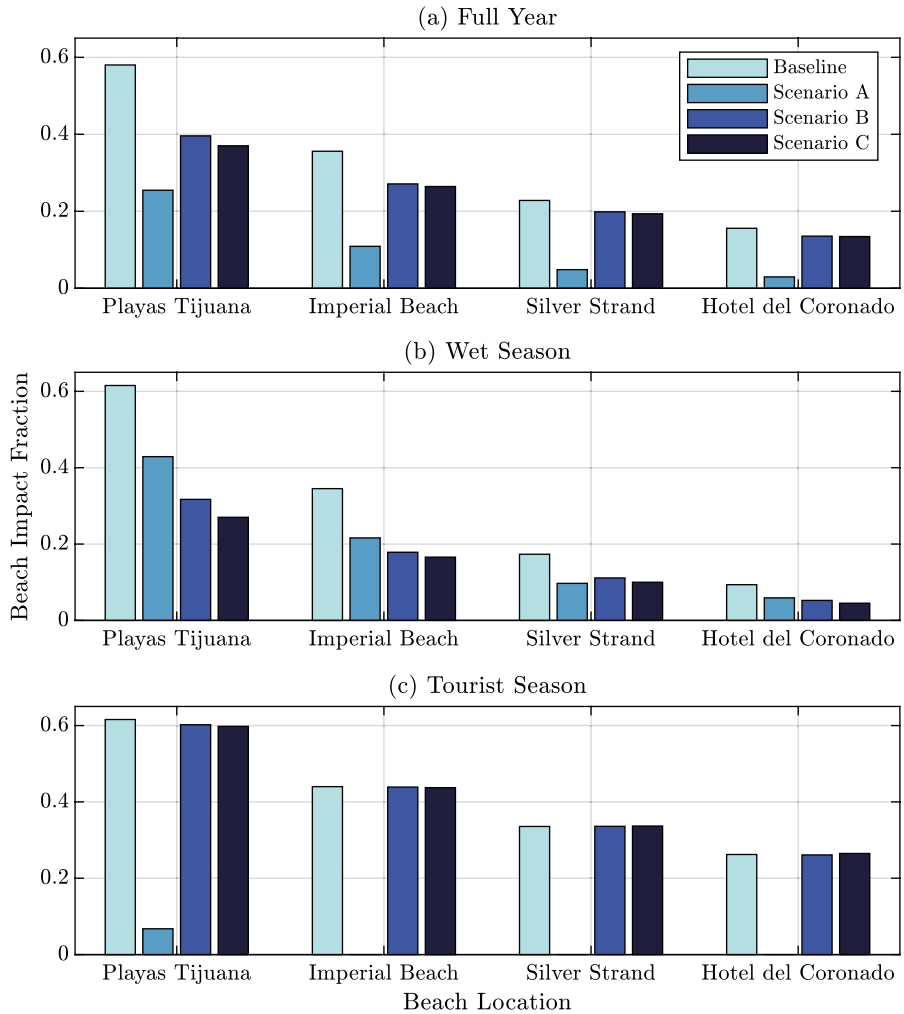


**Figure 8.** Beach impact fraction at the four beach locations for the four scenarios (legend) over the (a) full year, (b) wet season, and (c) tourist season. Beach impact fraction is defined as the fraction of time that $\tilde{P}^{\text{ill}} > P^{\text{ill}}_{\text{EPA}}$ ($P^{\text{ill}}_{\text{EPA}} = 0.036$, corresponding to $D = 1.06 \times 10^{-4}$). The locations Playas Tijuana, Imperial Beach, Silver Strand State Beach, and Hotel del Coronado are indicated in Figures 1, 4 and 5.

## 4. Discussion

### 4.1. Regional Beach Impacts Under the Four Scenarios

The EPA swimmer illness probability threshold $P^{\text{ill}}_{\text{EPA}} = 0.036$ is used to set recreational water quality criteria (USEPA, 2012). We define the beach impact fraction as the fraction of time that $\tilde{P}^{\text{ill}} > P^{\text{ill}}_{\text{EPA}}$. Here, we evaluate the beach impact fraction at four popular beaches PTJ, IB, SS, and HdC for the four scenarios over the full year, wet season, and tourist season (Figure 8). For the Baseline (first bar, Figure 8), PTJ is highly impacted at all three time-periods with beach impact fraction ≈ 0.6. This is because PTJ is closest to the dominant tourist season SAB/PTB source, which is downstream from the TJRE during the wet season with predominant NW-incident waves. Baseline beach impact fraction is steadily reduced northward with distance from SAB/PTB source but is still 0.35–0.44 at IB across seasons and even 0.26 at HdC during the tourist season (Figure 8) with northward flowing SAB/PTB plumes (e.g., Figure 4c). In Scenario A (second bar in Figure 8), tourist season beach impact fraction is dramatically reduced to 0.07 at PTJ and to zero at IB, SS, and HdC. In the wet season, Scenario A results in small wet season reductions at all locations, primarily from the October SAB/PTB plume events. During tourist season, Scenarios B and C (third and fourth bars, respectively, in Figure 8) have nearly identical beach impact fraction as the Baseline. During the wet season, Scenarios B and C reduce the beach impact fraction 1/2 to 1/3 relative to the Baseline depending on location.

**Table 4**
*Wet and Tourist Season Average Flow Rates $Q_f$ and Percentage of Time Flowing for 4 Years*

| | Wet season TJRE | | Tourist season TJRE | |
|---|---|---|---|---|
| Year | Average $Q_f$ | Percent time flowing | Average $Q_f$ | Percent time flowing |
| 2016–2017 | 139.8 MGD | 67% | 0.1 MGD | 2% |
| 2017–2018 | 19.1 MGD | 22% | 0 MGD | 0% |
| 2018–2019 | 88.5 MGD | 64% | 3.5 MGD | 14% |
| 2019–2020 | 139.4 MGD | 73% | 11.1 MGD | 79% |

*Note*. The percent time flowing is the percentage of time that the measured flow rate entering the TJRE is >2 MGD. Note, wet season is defined here continuously as (for 2016–2017) October 1, 2016 to April 1, 2017, and tourist season is defined as May 22 to September 8. TJRE, Tijuana River Estuary.

Scenario A provides the largest reduction in beach impact fraction over the full year and tourist season, but not the wet season (Figure 8). This is largely consistent with the $N_{ill}$ metric (Table 3), where Scenario A provided the largest reduction in all three time-periods. This difference is due to weighting the $N_{ill}$ metric by $N_{swim}$ and Fall having more swimmers than January–March (Figure 6b).

### 4.2. Contextualizing the Results

San Diego County performs weekly ENT sampling at IB and SS. During the 16-week long 2017 tourist season, the California single sample standard of 104 CFU/100 ml was only exceeded once at IB and not at all at SS (San Diego County, n. d.). In contrast, the Baseline $\bar{P}^{ill}$-based IB and SS beach impact fractions during tourist season were between 0.42 and 0.33, respectively (Figure 8). Differences in ENT and NoV decay, particularly under sunlit conditions, may explain the discrepant results. Daytime surfzone ENT inactivations time-scales were estimated at 0.05 days (Rippy et al., 2013) consistent with daylight river and seawater experiments of 0.025–0.23 days (Davies-Colley et al., 1994; Sinton et al., 2002). For SAB/PTB sourced untreated wastewater advecting at 10 km $d^{-1}$ (Figure 5) to IB, ENT would be exposed to at least 0.5 days of daylight and (assuming no night-time mortality) would be reduced purely from mortality a log10 factor of −1 to −4.4 ($0.11–4 \times 10^{-5}$). In contrast, with a 10-day decay time-scale, NoV is reduced a log10 factor −0.07. This neglects effects of hydrodynamic dilution. This suggests that the current advisory posting methods based on ENT might not be protective of swimmer health.

Our model results showing the effect of SAB/PTB plumes advecting northward are qualitatively consistent with the digital-PCR and DNA-sequenced microbial parameters measured from SAB/PTB, PTJ, IB, and SS during Fall 2018 south swell events (Zimmer-Faust et al., 2021). Human PCR markers, inferred to be sourced from SAB/PTB, were often detected at IB and SS. In contrast, elevated co-sampled ENT was never detected in IB and rarely at SS. The wet season Baseline $N_{ill}/N_{swim}$ can also be contextualized with epidemiological studies of increased illness risk in urban runoff (not untreated wastewater). At a beach (Mission Beach—MB—CA) ≈25 km north of IB, post rainfall exposure to ocean water with urban runoff increased the illness rate 0.7% relative to no swimming exposure for dominant GI illness as well as fever, eye infection, and wound infection (Arnold et al., 2017). During the wet season, IB NoV $N_{ill}/N_{swim}$ is 2.8% (Table 3), and predominant NoV symptoms are GI with fever secondary. Although difficult to compare epidemiological and our coupled model risk at different sites and time periods, their similar wet-season illness percentage (with MB factor 4 smaller), suggests that our coupled model is simulating a reasonable $N_{ill}/N_{swim}$.

### 4.3. Is the Year 2017 Representative?

The coupled San Diego Bight model applied in the year 2017 indicates that the SAB/PTB untreated wastewater source is the leading cause of swimmer illness and beach advisories. Therefore, reducing SAB/PTB discharges is expected to have the largest benefits in terms of coastal water quality and human health. However, the year 2017 (December 15, 2016 to December 15, 2017) conditions may not be representative of past or future conditions. Here, we examine the wet season and tourist season TJRE average inflow $Q_f$ and fraction of time flowing over four years (Table 4) using Tijuana River $Q_f$ (e.g., Figure 2a). The tourist season is defined as in Section 2 (22 May to 8 September). As multiple observation years are available, here we define wet season as 1 October to 1 April continuous, which differs from the Year 2017 wet season definition (December 15, 2016 to April 1, 2017 and October 1, 2017 to December 15, 2017—see Section 2).

The 2016–2017 wet season had the largest TJRE average $Q_f$ of 139.8 MGD and flowed 67% of the time (Table 4). The 2017–2018 wet season had much less TJRE average $Q_f$ (19.1 MGD) and only flowed 22% as the winter was drier. The 2018–2019 wet season TJRE average flow rate ($Q_f$ = 88.5 MGD) was ≈ 2/3 of the 2016–2017 wet season yet flowed at a similar rate (64%) as 2016–2017. The 2019–2020 wet season was most similar to 2016–2017 with TJRE average $Q_f$ of 139.4 MGD and flowed 73% of the time. The large TJRE $Q_f$

flows in 2016–2017 and 2019–2020 wet seasons are principally due to enhanced precipitation but is also partially due to failure of wastewater treatment and river diversion infrastructure in Tijuana (e.g., IBWC, 2017). Our model year 2017 wet season incorporated components of both the 2016–2017 (December 15, 2016 to April 1, 2017) and the 2017–2018 (October 1, 2017 to December 15, 2016) wet seasons and thus is largely representative of the range of wet season conditions. In addition, the early wet season (December 15, 2016 to April 1, 2017) is representative of the largest $Q_f$ flow conditions over the 4 years. How the untreated wastewater inflow $Q_D$ changes across these four wet seasons is unknown as it depends on Tijuana infrastructure, although likely $Q_D$ is monotonic with $Q_f$.

The 2017 tourist season had low TJRE average $Q_f$ of 0.1 MGD and flowed 2% of the time, explaining why SAB/PTB had much larger tourist season impacts (Figures 5, 6 and 8 and Table 3). However, the 2017 tourist season is not representative of more recent tourist season TJRE inflows (Table 4). The 2018 tourist season had even less TJRE flows, suggesting our tourist season conclusions apply. However, tourist season TJRE inflows increased in 2019 and 2020 with average $Q_f$ of 3.5 MGD to 11.1 MGD, respectively, with 2020 flow frequency increasing to 79% (Table 4). Aside from one small 2 mm precipitation event on June 20, 2020, the year 2020 tourist season was dry (NCEI-NOAA, n.d.). Thus, the strong 2020 tourist season TJRE inflows were due to ongoing (November 2019 through September 2020) Tijuana wastewater and river diversion infrastructure failure, indicating the TJRE inflow is largely untreated wastewater, that is, $Q_D \approx Q_f$. The IB pier is 2.9 km from the TJRE relative to 15 km from SAB/PTB (Figure 1). During the 2020 tourist season, a TJRE $Q_D$ 1/3 that of SAB/PTB would likely result in larger $D$ and associated increases swimmer illness risk from the TJRE than from SAB/PTB at IB and farther northward. Note, SAB/PTB impacts would still be present, similar to 2017. The 2019 tourist season also likely has significant yet intermittent TJRE impacts. Thus, our 2017 tourist season Baseline results may not be representative of other years or of the future. However, the 2020 TJRE tourist season $Q_f$ was almost always <35 MGD, suggesting that Scenario A, which diverts TJRE inflows <35 MGD, is still the optimal scenario for improving shoreline water quality. These inferences assume that tourist season net south swell energy does not vary substantially across years.

### 4.4. Limitations

The $N_{\text{ill}}$ and beach impact fraction for each scenario are based on a cascade of inputs and coupled model components. Each model component has been separately developed and tested (e.g., Boehm & Soller, 2020; Kumar et al., 2012, and references therein). Yet, the many assumptions and choices here have limitations, of which we enumerate a few. First, the hydrodynamics are wave-averaged and do not include stirring due to transient rip currents (e.g., Suanda & Feddersen, 2015) which may dilute the shoreline more rapidly than modeled. The TJRE source flow rates ($Q_f$) are based on the IBWC flow gauge, but the flow of untreated wastewater ($Q_D$) was not measured and is likely more variable and complex than our simple assumptions. In addition, TJRE untreated wastewater inputs downstream of the IBWC flow gauge (e.g., Goat and Yogurt Canyons) occasionally occur with rainfall with unknown magnitude and are not included here. We only model a single pathogen NoV whose data on surface water persistence is limited. The decay time-scale value used herein represents the best estimate to date. Although NoV dominates risk when swimmers are exposed to fresh or aged untreated wastewater contamination (e.g., Schoen et al., 2020), ill swimmers can be infected by a range of pathogens (Dorevitch et al., 2012). More complex tracer modeling is required to include additional pathogens. The swimmer ingested water volume probability distribution (DeFlorio-Barker, Arnold, et al., 2018) did not consider surfers whose exposure duration and thus volume ingested is likely larger than a typical recreational swimmer. Both SAB/PTB and TJRE have the same time-stationary source NoV concentration $C_{\text{src}}$ based on measurements of treatment plant inflow. We do not consider NoV decay during the transit to the TJRE or SAB/PTB discharge locations. However,the decay is expected to be minor as the transit time is likely <0.5 days (relative to the 10-day decay time-scale) for both sources based on Tijuana wastewater infrastructure (ARCADIS, 2019). A real swimmer draws only one local NoV concentration, whereas we ensemble average over the NoV source concentration $C_{\text{src}}$ distribution, which gives greater statistical reliability but may misrepresent sample variability. The $N_{\text{swim}}$ only vary over a month (Figure 6b) and not within a week or day. In Appendix A, we show that intra-day variations of $N_{\text{swim}}$ do not affect the results and discuss potential effects of intra-week variations. Swimmer behavior ($N_{\text{swim}}$) does not change under the different scenarios, whereas a feedback between water quality and swimmer behavior might be expected.

For February, 10% of beach visitors become swimmers following Given et al. (2006). However, this may not account for the nearly 100% likelihood of a surfer visiting the beach becoming a swimmer in winter months.

## 5. Summary

Here, we developed a coupled hydrodynamic, NoV pathogen, and QMRA swimmer illness risk model that spans estuary, surfzone, and shelf. This model is applied to the San Diego Bight (US/MX border region) which has two untreated wastewater sources to the ocean—the TJRE, whose mouth is 2 km north of the border, and the SAB outfall discharging at the ocean shoreline at PTB (SAB/PTB), 10 km south of the border—that lead to human health and beach impacts. We simulate the year 2017 under four scenarios that include a Baseline (no change) and three infrastructure diversion scenarios (A, B, C) that represent the range of potential projects funded under the US-Mexico-Canada trade agreement. Scenario A strongly reduces the SAB/PTB source and moderately reduces the TJRE source. Scenarios B and C strongly reduce the TJRE source only. Analysis is performed over the tourist season (late May to early September), wet season (1 October to 1 April), and over the full year. In wet season, the TJRE is the dominant source to the San Diego Bight whereas SAB/PTB is the dominant source in tourist season.

The untreated wastewater has distinct wet and tourist season transport and dilution pathways in the San Diego Bight. In particular, south swell events (consistent swell incident from the south) drive plumes of SAB/PTB-sourced untreated wastewater north at rates of ~10 km $d^{-1}$, that can impact the entire shoreline of the Bight. These plumes are largely removed in Scenario A. Using beach visitor data, we simulate the number of ill swimmers at IB CA under the four scenarios. In the Baseline, 3.8% of yearly swimmers are estimated to become ill, increasing to 4.5% during the tourist season due to the south-swell driven plumes from SAB/PTB. Scenario A leads to the largest reduction in ill swimmers. We show that using the mean ill probability based on untreated wastewater concentration results in good estimates of ill swimmers, allowing estimation of the fractional time that regional beaches are impacted. Under the Baseline, regional beaches are significantly impacted with weaker impacts farther north, and Scenario A yields the largest reduction in beach impacts overall. The 2017 tourist inflows may not be representative of other years, yet Scenario A still provides the greatest benefit for other years. Although the modeling approach has limitations, it is the first time hydrodynamic, pathogen, and human illness models have been coupled to predict human health and beach impacts. This methodology can be applied to other coastal regions with wastewater inputs.

## Appendix A: Effect of Daily Beach Swimmer Variation

To estimate $N_{ill}$ (Section 3.3), hourly beach swimmers $N_{swim}$ only varied monthly as the IB beach visitor data, used to estimate $N_{swim}$ (Given et al., 2006), was compiled monthly. Beach visitor data was not broken down to day of the week or hour of the day. Obviously more swimmers are present at noon than at midnight, and there are likely more swimmers on a Tuesday than a Saturday. This is not considered in determining $N_{ill}$, as methods for distributing beach visitors intra-week or intra-day do not exist. In Section 3.3, intra-day and week variations in $N_{swim}$ were argued to not be important in determining yearly, wet season, or tourist season number of ill swimmer $N_{ill}$ as the random plume occurrence across day and night would average out across the net number of swimmers.

We can test the effect of intra-day variations by applying a weight $w(t)$ to the $N_{swim}$ time-series where $w(t)$ incorporates a simple intra-day solar radiation variation of

$$w(t) = \begin{cases} W^{-1}\cos\left[\frac{(t_{hr}-12\ \mathrm{h})\pi}{12\ \mathrm{h}}\right], & 6 < t_{hr} < 18\ \mathrm{h} \\ 0, & \text{otherwise} \end{cases}, \tag{A1}$$

where $t_{hr}$ is the decimal hour of the day and $W$ is set so the daily integral of Equation A1 is one. This weight has maximum swimmers at noon local (12:00) and no swimmers between 18:00 and 06:00. Note, Equation A1 does not include seasonal variations in day-length, nor are intra-week variations in $N_{swim}$ considered. We define a new hourly swimmer timeseries $\tilde{N}_{swim}(t) = w(t)N_{swim}(t)$ and use it within the illness risk model to estimate yearly, wet season, and tourist season $\tilde{N}_{ill}$ for the four scenarios.

Over the full year, wet season and tourist season, the percentage of ill swimmers from $\tilde{N}_{ill}$ (Table A1) based on intra-day swimmer variations is essentially unchanged from $N_{ill}$ that neglects intra-day swimmer variations (Table 3). The largest percentage difference between $\tilde{N}_{ill}$ and $N_{ill}$ is 0.1%. Although within a specific day $N_{ill}$ and $\tilde{N}_{ill}$ differ, the seasonal similarity $\tilde{N}_{ill}$ and $N_{ill}$ is because the duration of untreated wastewater events is generally greater than a day (Figure 4). Most events though are shorter than a week and so intra-week swimmer variations may yield weekly $N_{ill}$ variations. But the 16 weeks of tourist season potentially averages this out as well.

**Table A1**
*Ill Swimmer $\tilde{N}_{ill}$ Percentage When Included Intra-Day Variations in Swimmer Number $\tilde{N}_{swim}$ (Equation A1) at Imperial Beach CA Under the Four Scenarios for the (Columns) Full Year, Wet Season, and Tourist Season*

| | Ill swimmers $\tilde{N}_{ill}$ percentage of $N_{swim}$ | | |
|---|---|---|---|
| Scenario | Full year | Wet season | Tourist season |
| Baseline | 3.8% | 2.9% | 4.5% |
| Scenario A | 0.6% | 1.2% | 0.5% |
| Scenario B | 3.7% | 2.3% | 4.5% |
| Scenario C | 3.7% | 2.2% | 4.5% |

*Note*. These values should be compared to the $N_{ill}$ percentages in Table 3.

**Acknowledgments**
This work was funded by the Environmental Protection Agency through the North American Development Bank. However, it does not necessarily reflect the policies, actions or positions of the U.S. EPA or NADB. This work was also supported by the National Science Foundation (OCE-1459389) as part of the Cross-Surfzone/Inner-shelf Dye Exchange (CSIDE) experiment. This project is supported, in part, by the US Coastal Research Program (USCRP) as administered by the US Army Corps of Engineers (USACE), Department of Defense and in part by NSF OCE-1924005. The content of the information provided in this publication does not necessarily reflect the position or the policy of the government, and no official endorsement should be inferred. The authors' acknowledge the USACE and USCRP's support of their effort to strengthen coastal academic programs and address coastal community needs in the United States. The City of Imperial Beach provided the beach visitor data. NOAA provided the hydrodynamic model atmospheric forcing fields and the bathymetry. SIO Coastal Data Information Program provided wave forcing. Ganesh Gopalakrishnan and Bruce Cornuelle provided CASE model solutions for outer grid boundary conditions which are available online (http://ecco.ucsd.edu/case.html). We also appreciate extra support from the Tijuana River National Estuarine Research Reserve and the Southern California Coastal Ocean Observing System. Derek Grimes and Elizabeth Brasseale provided useful feedback on this work.

## Conflict of Interest

The authors declare no conflicts of interest relevant to this study.

## Data Availability Statement

The shoreline $D$ data set can be accessed via zenodo.org at https://doi.org/10.5281/zenodo.5056617 (Feddersen et al., 2021).

## References

ARCADIS. (2019). *Tijuana river diversion study* (Technical report). North American Development Bank. Retrieved from https://www.nadb.org/uploads/files/tijuana_river_diversion_study_final_report_full_sm.pdf

Arnold, B. F., Schiff, K. C., Ercumen, A., Benjamin-Chung, J., Steele, J. A., Griffith, J. F., et al. (2017). Acute illness among surfers after exposure to seawater in dry- and wet-weather conditions. *American Journal of Epidemiology*, *186*(7), 866–875. https://doi.org/10.1093/aje/kwx019

Ayad, M., Li, J., Holt, B., & Lee, C. (2020). Analysis and classification of stormwater and wastewater runoff from the Tijuana River using remote sensing imagery. *Frontiers in Environmental Science*, *8*, 240. https://doi.org/10.3389/fenvs.2020.599030

Boehm, A. B., Silverman, A. I., Schriewer, A., & Goodwin, K. (2019). Systematic review and meta-analysis of decay rates of waterborne mammalian viruses and coliphages in surface waters. *Water Research*, *164*, 114898. https://doi.org/10.1016/j.watres.2019.114898

Boehm, A. B., & Soller, J. (2020). Refined ambient water quality thresholds for human-associated fecal indicator HF183 for recreational waters with and without co-occurring gull fecal contamination. *Microbial Risk Analysis*, *16*, 100139. https://doi.org/10.1016/j.mran.2020.100139

Boehm, A. B., Soller, J. A., & Shanks, O. C. (2015). Human-associated fecal quantitative polymerase chain reaction measurements and simulated risk of gastrointestinal illness in recreational waters contaminated with raw sewage. *Environmental Science and Technology Letters*, *2*(10), 270–275. https://doi.org/10.1021/acs.estlett.5b00219

Booij, N., Ris, R. C., & Holthuijsen, L. H. (1999). A third-generation wave model for coastal regions: 1. Model description and validation. *Journal of Geophysical Research*, *104*(C4), 7649–7666. https://doi.org/10.1029/98JC02622

Brophy, T. (2016). *Environmental and community health in south San Diego County: A behavior analysis of recreational ocean users along Imperial Beach, California* (Unpublished master's thesis, Graduate Theses and Dissertations). University of South Florida. Retrieved from http://scholarcommons.usf.edu/etd/6186

Davies-Colley, R. J., Bell, R. G., & Donnison, A. M. (1994). Sunlight inactivation of enterococci and fecal coliforms in sewage effluent diluted in seawater. *Applied and Environmental Microbiology*, *60*(6), 2049–2058. https://doi.org/10.1128/aem.60.6.2049-2058.1994

DeFlorio-Barker, S., Arnold, B., Sams, E., Dufour, A. P., Colford, J. M., Weisberg, S. B., et al. (2018). Child environmental exposures to water and sand at the beach: Findings from studies of over 68,000 subjects at 12 beaches. *Journal of Exposure Science and Environmental Epidemiology*, *28*, 93–100. https://doi.org/10.1038/jes.2017.23

DeFlorio-Barker, S., Wing, C., Jones, R. M., & Dorevitch, S. (2018). Estimate of incidence and cost of recreational waterborne illness on United States surface waters. *Environmental Health*, *17*. https://doi.org/10.1186/s12940-017-0347-9

Dorevitch, S., Dworkin, M. S., DeFlorio, S. A., Janda, W. M., Wuellner, J., & Hershow, R. C. (2012). Enteric pathogens in stool samples of Chicago-area water recreators with new-onset gastrointestinal symptoms. *Water Research*, *46*(16), 4961–4972. https://doi.org/10.1016/j.watres.2012.06.030

Eftim, S. E., Hong, T., Soller, J., Boehm, A., Warren, I., Ichida, A., & Nappier, S. P. (2017). Occurrence of norovirus in raw sewage—Systematic literature review and meta-analysis. *Water Research*, *111*, 366–374. https://doi.org/10.1016/j.watres.2017.01.017

Feddersen, F., Olabarrieta, M., Guza, R. T., Winters, D., Raubenheimer, B., & Elgar, S. (2016). Observations and modeling of a tidal inlet dye tracer plume. *Journal of Geophysical Research: Oceans*, *121*, 7819–7844. https://doi.org/10.1002/2016JC011922

Feddersen, F., Wu, X., & Giddings, S. N. (2021). *Modeled San Diego Bight shoreline untreated wastewater concentration for year 2017*. [Data set] Zenodo.org. https://doi.org/10.5281/zenodo.5056617

Feng, Z., Reniers, A., Haus, B. K., & Solo-Gabriele, H. M. (2013). Modeling sediment-related enterococci loading, transport, and inactivation at an embayed nonpoint source beach. *Water Resources Research*, *49*(2), 693–712. https://doi.org/10.1029/2012WR012432

Fleisher, J. M., Kay, D., Salmon, R. L., Jones, F., Wyer, M. D., & Godfree, A. F. (1996). Marine waters contaminated with domestic sewage: Nonenteric illnesses associated with bather exposure in the United Kingdom. *American Journal of Public Health*, *86*(9), 1228–1234. https://doi.org/10.2105/AJPH.86.9.1228

Given, S., Pendleton, L. H., & Boehm, A. B. (2006). Regional public health cost estimates of contaminated coastal waters: A case study of gastroenteritis at Southern California beaches. *Environmental Science and Technology*, *40*(16), 4851–4858. https://doi.org/10.1021/es060679s

Grant, S. B., Kim, J. H., Jones, B. H., Jenkins, S. A., Wasyl, J., & Cudaback, C. (2005). Surf zone entrainment, along-shore transport, and human health implications of pollution from tidal outlets. *Journal of Geophysical Research*, *110*, C10025. https://doi.org/10.1029/2004JC002401

Grimes, D. J., Feddersen, F., & Giddings, S. N. (2021). Long-distance/time surf-zone tracer evolution affected by inner-shelf tracer retention and recirculation. *Journal of Geophysical Research: Oceans*. https://doi.org/10.1029/2021jc017661

Grimes, D. J., Feddersen, F., Giddings, S. N., & Pawlak, G. (2020). cross-shore deformation of a surfzone-released dye plume by an internal tide on the inner shelf. *Journal of Physical Oceanography*, *50*(1), 35–54. https://doi.org/10.1175/JPO-D-19-0046.1

Haile, R. W., Witte, J. S., Gold, M., Cressey, R., McGee, C. D., Millikan, R. C., et al. (1999). The health effects of swimming in ocean water contaminated by storm drain runoff. *Epidemiology*, *10*, 355–363. https://doi.org/10.1097/00001648-199907000-00004

Hally-Rosendahl, K., Feddersen, F., Clark, D. B., & Guza, R. T. (2015). Surfzone to inner-shelf exchange estimated from dye tracer balances. *Journal of Geophysical Research: Oceans*, *120*, 6289–6308. https://doi.org/10.1002/2015JC010844

IBWC, M. B. T. T. W. Q. W. (2017). *Report of transboundary bypass flows into the Tijuana River study* (Technical report). International Boundary and Water Commission United States and Mexico. Retrieved from https://www.ibwc.gov/Files/Report_Trans_Bypass_Flows_Tijuana_033117.pdf

IBWC-Data. (n.d.). *Tijuana River at international boundary flow gauge station*. Retrieved from https://waterdata.ibwc.gov/Data/Location/Summary/Location/11013300/Interval/Latest

Johnson, A. E., Powell, B. S., & Steward, G. F. (2013). Characterizing the effluence near Waikiki, Hawaii with a coupled biophysical model. *Continental Shelf Research*, *54*, 1–13. https://doi.org/10.1016/j.csr.2012.12.007

Kastner, S. E., Horner-Devine, A. R., & Thomson, J. M. (2019). A conceptual model of a river plume in the surf zone. *Journal of Geophysical Research: Oceans*, *124*(11), 8060–8078. https://doi.org/10.1029/2019JC015510

Kim, S. Y., Terrill, E. J., & Cornuelle, B. D. (2009). Assessing coastal plumes in a region of multiple discharges: The US-Mexico border. *Environmental Science & Technology*, *43*(19), 7450–7457. https://doi.org/10.1021/es900775p

Kumar, N., Feddersen, F., Uchiyama, Y., McWilliams, J. C., & O'Reilly, W. (2015). Midshelf to surfzone coupled ROMS-SWAN model data comparison of waves, currents, and temperature: Diagnosis of subtidal forcings and response. *Journal of Physical Oceanography*, *45*, 1464–1490. https://doi.org/10.1175/JPO-D-14-0151.1

Kumar, N., Voulgaris, G., Warner, J. C., & Olabarrieta, M. (2012). Implementation of the vortex force formalism in the coupled ocean-atmosphere-wave-sediment transport (COAWST) modeling system for inner shelf and surf zone applications. *Ocean Modelling*, *47*(0), 65–95. https://doi.org/10.1016/j.ocemod.2012.01.003

Lahet, F., & Stramski, D. (2010). Modis imagery of turbid plumes in San Diego coastal waters during rainstorm events. *Remote Sensing of Environment*, *114*(2), 332–344. https://doi.org/10.1016/j.rse.2009.09.017

Liu, L., Phanikumar, M. S., Molloy, S. L., Whitman, R. L., Shively, D. A., Nevers, M. B., et al. (2006). Modeling the transport and inactivation of *E. coli* and enterococci in the near-shore region of Lake Michigan. *Environmental Science & Technology*, *40*(16), 5022–5028. https://doi.org/10.1021/es060438k

Madani, M., Seth, R., Leon, L. F., Valipour, R., & McCrimmon, C. (2020). Three dimensional modelling to assess contributions of major tributaries to fecal microbial pollution of lake St. Clair and Sandpoint Beach. *Journal of Great Lakes Research*, *46*(1), 159–179. https://doi.org/10.1016/j.jglr.2019.12.005

NCEI-NOAA (n.d.). San Diego International Airport Station details. Retrieved from https://www.ncdc.noaa.gov/cdo-web/datasets/GHCND/stations/GHCND:USW00023188/detail

Olabarrieta, M., Geyer, R., & Kumar, N. (2014). The role of morphology and wave-current interaction at tidal inlets: An idealized modeling analysis. *Journal of Geophysical Research: Oceans*, *119*, 8818–8837. https://doi.org/10.1002/2014JC010191

Olabarrieta, M., Warner, J. C., & Kumar, N. (2011). Wave-current interaction in Willapa Bay. *Journal of Geophysical Research*, *116*(C12). https://doi.org/10.1029/2011JC007387

Orozco-Borbón, M. V., Rico-Mora, R., Weisberg, S. B., Noble, R. T., Dorsey, J. H., Leecaster, M. K., & McGee, C. D. (2006). Bacteriological water quality along the Tijuana–Ensenada, Baja California, México shoreline. *Marine Pollution Bulletin*, *52*(10), 1190–1196. https://doi.org/10.1016/j.marpolbul.2006.02.005

Pouillot, R., Van Doren, J. M., Woods, J., Plante, D., Smith, M., Goblick, G., et al. (2015). Meta-analysis of the reduction of norovirus and male-specific coliphage concentrations in wastewater treatment plants. *Applied and Environmental Microbiology*, *81*(14), 4669–4681. https://doi.org/10.1128/AEM.00509-15

Rippy, M. A., Franks, P. J. S., Feddersen, F., Guza, R. T., & Moore, D. F. (2013). Factors controlling variability in nearshore fecal pollution: The effects of mortality. *Marine Pollution Bulletin*, *66*(1–2), 191–198. https://doi.org/10.1016/j.marpolbul.2012.09.003

Rodriguez, A. R., Giddings, S. N., & Kumar, N. (2018). Impacts of nearshore wave-current interaction on transport and mixing of small-scale buoyant plumes. *Geophysical Research Letters*, *45*(16), 8379–8389. https://doi.org/10.1029/2018GL078328

San Diego County (n. d.). San Diego Beach information. Retrieved from http://www.sdbeachinfo.com/

Sano, D., Amarasiri, M., Hata, A., Watanabe, T., & Katayama, H. (2016). Risk management of viral infectious diseases in wastewater reclamation and reuse: Review. *Environment International*, *91*, 220–229. https://doi.org/10.1016/j.envint.2016.03.001

Sassoubre, L. M., Love, D. C., Silverman, A. I., Nelson, K. L., & Boehm, A. B. (2012). Comparison of enterovirus and adenovirus concentration and enumeration methods in seawater from Southern California, USA and Baja Malibu, Mexico. *Journal of Water and Health*, *10*(3), 419–430. https://doi.org/10.2166/wh.2012.011

Schoen, M. E., & Ashbolt, N. J. (2010). Assessing pathogen risk to swimmers at non-sewage impacted recreational beaches. *Environmental Science & Technology*, *44*(7), 2286–2291. https://doi.org/10.1021/es903523q

Schoen, M. E., Boehm, A. B., Soller, J., & Shanks, O. C. (2020). Contamination scenario matters when using viral and bacterial human-associated genetic markers as indicators of a health risk in untreated sewage-impacted recreational waters. *Environmental Science & Technology*, *54*(20), 13101–13109. https://doi.org/10.1021/acs.est.0c02189

Shchepetkin, A. F., & McWilliams, J. C. (2005). The regional oceanic modeling system (ROMS): A split-explicit, free-surface, topography-following-coordinate oceanic model. *Ocean Modelling*, *9*(4), 347–404. https://doi.org/10.1016/j.ocemod.2004.08.002

Shuval, H. (2003). Estimating the global burden of thalassogenic diseases: Human infectious diseases caused by wastewater pollution of the marine environment. *Journal of Water and Health*, *1*, 53–64. https://doi.org/10.2166/wh.2003.0007

Sinton, L. W., Hall, C. H., Lynch, P. A., & Davies-Colley, R. J. (2002). Sunlight inactivation of fecal indicator bacteria and bacteriophages from waste stabilization pond effluent in fresh and saline waters. *Applied and Environmental Microbiology*, *68*(3), 1122–1131. https://doi.org/10.1128/AEM.68.3.1122-1131.2002

Suanda, S. H., & Feddersen, F. (2015). A self-similar scaling for cross-shelf exchange driven by transient rip currents. *Geophysical Research Letters*, *42*(13), 5427–5434. https://doi.org/10.1002/2015GL063944

Teunis, P. F., Moe, C. L., Liu, P., Miller, E. S., Lindesmith, L., Baric, R. S., et al. (2008). Norwalk virus: How infectious is it? *Journal of Medical Virology*, *80*(8), 1468–1476. https://doi.org/10.1002/jmv.21237

USEPA. (n.d.). *Improving water quality in the Tijuana River valley—Overview of projects*. Retrieved from https://www.epa.gov/sites/production/files/2021-04/documents/tijuana_valley-overview-final.pdf

USEPA. (2012). *Recreational water quality criteria* (Technical report, Vol. *820-F-12-058*).

USEPA. (n. d.). *National pollutant discharge elimination system*. Retrieved from https://www.epa.gov/npdes

Warner, J. C., Armstrong, B., He, R., & Zambon, J. B. (2010). Development of a coupled ocean-atmosphere-wave-sediment transport (COAWST) modeling system. *Ocean Modelling*, *35*(3), 230–244. https://doi.org/10.1016/j.ocemod.2010.07.010

Warrick, J., DiGiacomo, P., Weisberg, S., Nezlin, N., Mengel, M., Jones, B., et al. (2007). River plume patterns and dynamics within the southern California bight. *Continental Shelf Research*, *27*(19), 2427–2448. https://doi.org/10.1016/j.csr.2007.06.015

Weiskerger, C. J., & Phanikumar, M. S. (2020). Numerical modeling of microbial fate and transport in natural waters: Review and implications for normal and extreme storm events. *Water*, *12*(7), 1876. https://doi.org/10.3390/w12071876

Wong, S. H. C., Monismith, S. G., & Boehm, A. B. (2013). Simple estimate of entrainment rate of pollutants from a coastal discharge into the surf zone. *Environmental Science & Technology*, *47*(20), 11554–11561. https://doi.org/10.1021/es402492f

Wu, X., Feddersen, F., & Giddings, S. N. (2021a). Characteristics and dynamics of density fronts over the inner to mid-shelf under weak wind conditions. *Journal of Physical Oceanography*, *51*, 789–808. https://doi.org/10.1175/JPO-D-20-0162.1

Wu, X., Feddersen, F., & Giddings, S. N. (2021b). Diagnosing surfzone impacts on inner-shelf flow spatial variability using realistic model experiments with and without surface gravity waves. *Journal of Physical Oceanography*, *51*(8), 2505–2515. https://doi.org/10.1175/JPO-D-20-0324.1

Wu, X., Feddersen, F., Giddings, S. N., Kumar, N., & Gopalakrishnan, G. (2020). Mechanisms of mid- to outer-shelf transport of shoreline-released tracers. *Journal of Physical Oceanography*, *50*(7), 1813–1837. https://doi.org/10.1175/JPO-D-19-0225.1

Zimmer-Faust, A. G., Steele, J. A., Xiong, X., Staley, C., Griffith, M., Sadowsky, M. J., et al. (2021). A combined digital PCR and next generation DNA-sequencing based approach for tracking nearshore pollutant dynamics along the southwest U.S/Mexico border. *Frontiers in Microbiology*, *12*. https://doi.org/10.3389/fmicb.2021.674214